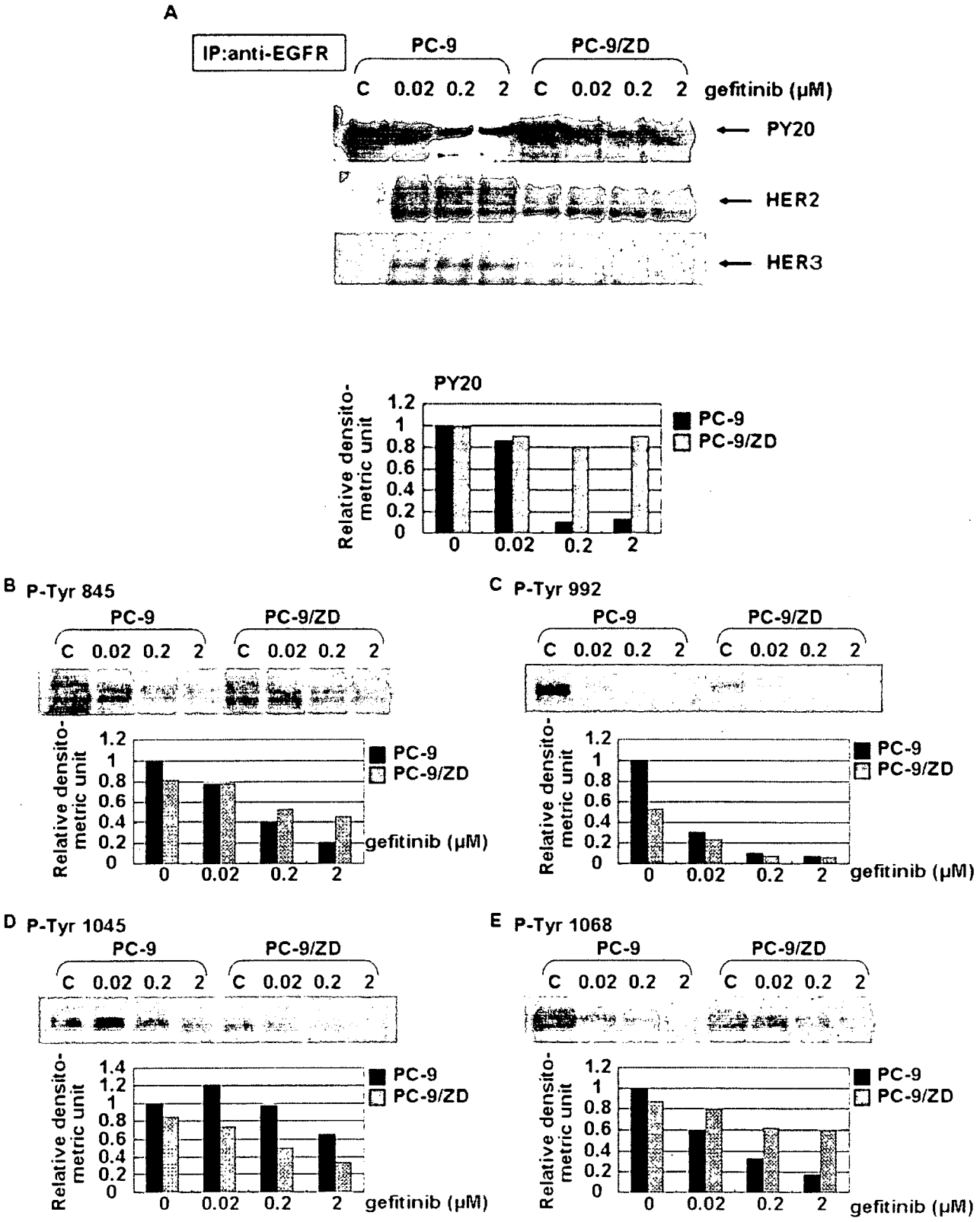

FIGURE 5 – Effect of gefitinib on autophosphorylation of EGFR. (*a*) PC-9 and PC-9/ZD cells (5×10^6) were exposed to 0.02, 0.2 or 2 μM gefitinib for 6 hr. The 1,500 μg of total cell lysate was immunoprecipitated with an anti-EGFR antibody. The immunoprecipitates were subjected to gel electrophoresis and Western blotting with anti-phosphotyrosine, anti-HER2 and anti-HER3 antibodies. Tyrosine-phosphorylated EGFR was determined with an anti-phosphotyrosine antibody. Heterodimer formation of EGFR was analyzed with anti-HER2 and anti-HER3 antibodies. The expression levels have been plotted in a graph. (*b–e*) PC-9 and PC-9/ZD cells were exposed to 0.02, 0.2 and 2 μM gefitinib for 6 hr. A 20 μg of protein of each sample was analyzed by Western blotting by using anti phospho-EGFR (Tyr845, Tyr992, Tyr 1045, Tyr 1068) antibodies.

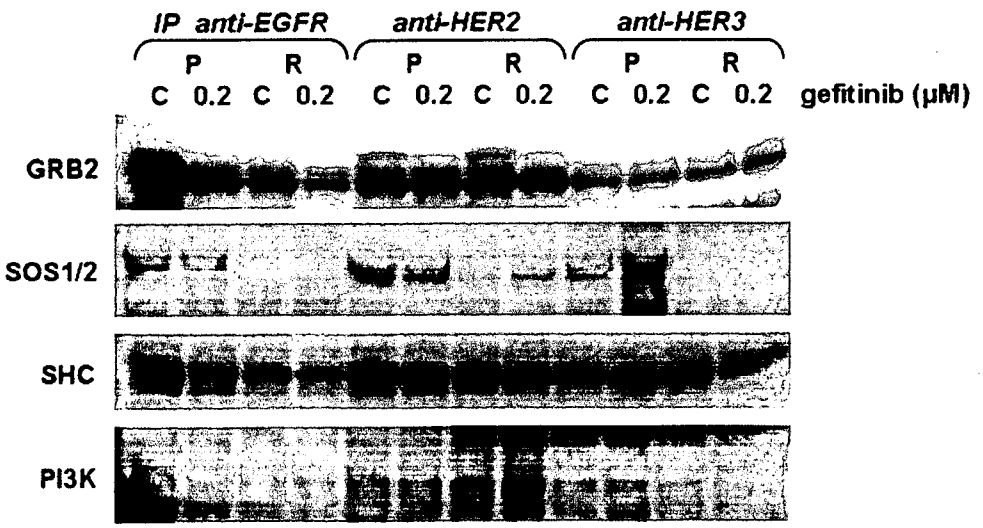

FIGURE 6 – Protein interaction between EGFR and its adaptor proteins. Cells (P: PC-9, R: PC-9/ZD) were exposed to 0 and 0.2 μM of gefitinib for 6 hr. The cells were lysed and immunoprecipitated with ant-EGFR, anti-HER2, and anti-HER3 antibodies, and the amounts of the Grb2, SOS1/2, SHC and PI3K precipitated were monitored by immunoblotting with their specific Abs.

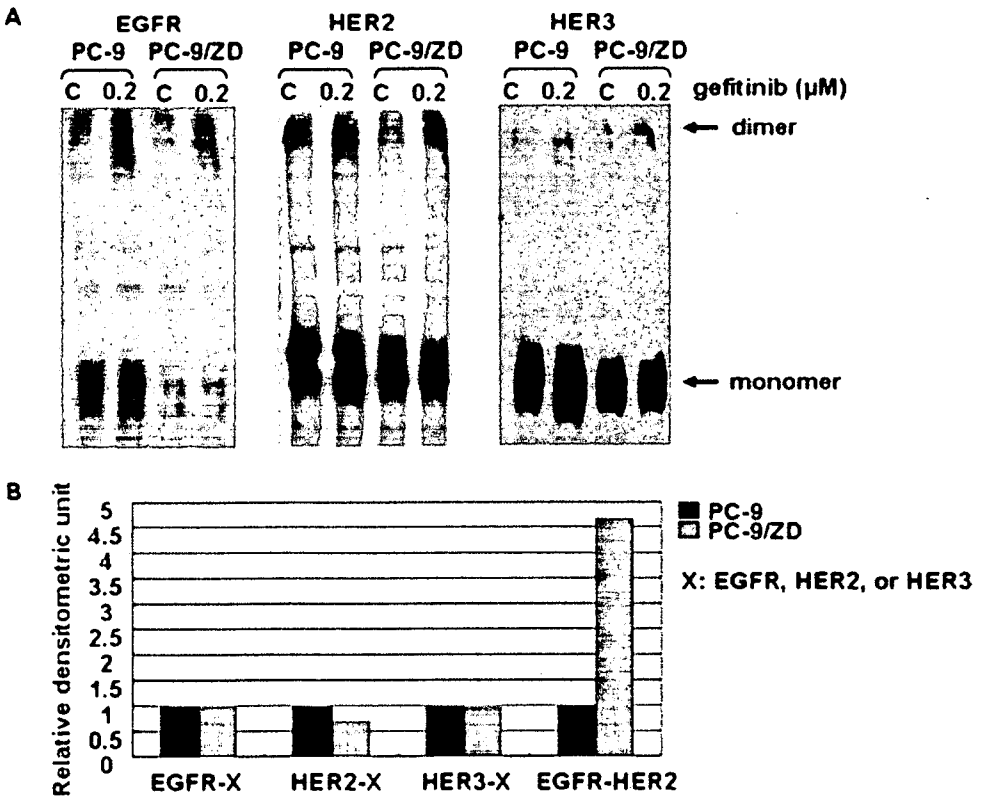

FIGURE 7 – Chemical cross-linking of PC-9 and PC-9/ZD cells. (*a*) After 6 hr exposure to 1.5 mM bis (sulfosuccinimidyl) substrate dissolved in PBS as indicated in Material and Methods. The cross-linking reaction was quenched and the cell lysates were prepared and subjected to immunoblot analysis of EGFR, HER2 and HER3. (*b*) Ratio of dimmers formed by PC-9 cells to those by PC-9/ZD cells in the absence of gefitinib. The density of the bands in (*a*) for EGFR-X, HER2-X and HER3-X were quantified densitometrically. The ratio of EGFR-HER2 was calculated by the band density obtained in Figure 5*a*. X = EGFR, HER2 or HER3.

Discussion

Interest in resistance to target-based therapy (TBT) has been growing ever since clinical efficacy was first demonstrated.[11–13] Although CML patients respond to STI-571 well at first, most patients eventually relapse in the late stage of the disease.[25–27] It has been reported that some patients in whom treatment with gefitinib is effective at first, ultimately become refractory.[30] Resistance is likely to remain a hurdle that limits the long-term effectiveness of TBT. PC-9 had a deletion mutation within the kinase domain of *EGFR* and is highly sensitive. These characters are similar to those of NSCLC with clinical responsiveness to gefitinib. Analyzing the mechanism of resistance of PC-9/ZD subline might be clinically meaningful.

The mechanism of drug resistance is thought to be multifactorial. Because the growth-inhibitory assay in our present study showed no cross resistance to a variety of cytotoxic agents, the mechanism of the resistance differs from the mechanism of multidrug resistance patterns. Although expression of BCRP, one of the multidrug-resistance-related proteins has been reported to contribute to the resistance to gefitinib,[31] expression of *BCRP* mRNA is observed only in PC-9 cells (data not shown). Although mutations in the ATP-binding pocket of *BCR-ABL* gene have been identified recently in cells from CML patients who were refractory to STI-571 treatment or relapse,[25–27] there have been no reports of any such mutations for gefitinib resistance. PC-9/ZD also became refractory to gefitinib without secondary mutation in *EGFR* cDNA. These suggest the possibility of refractory tumor after treatment of gefitinib including this kind of phenotype.

There is no significant difference in expression level of EGFR between PC-9 and PC-9/ZD. Does the antitumor effect of gefitinib

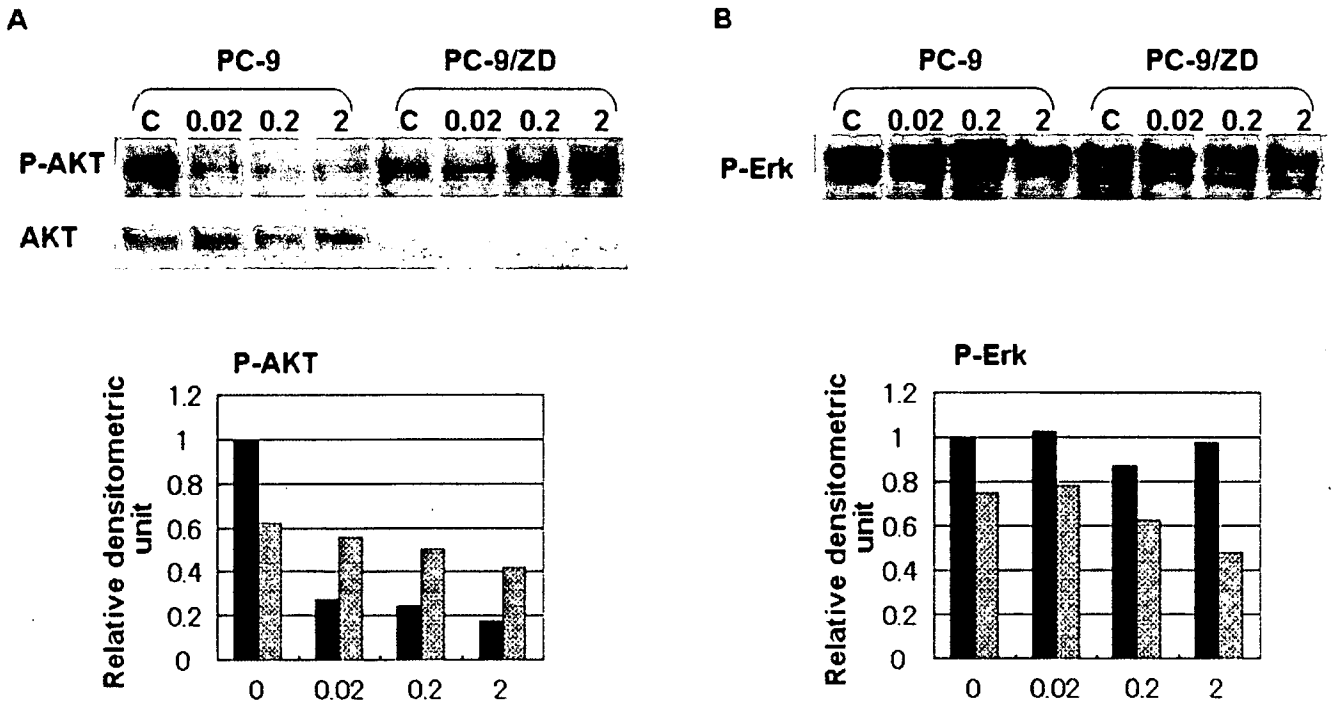

FIGURE 8 – Effect of gefitinib on the MAPK and AKT pathway. Cells were placed in medium containing 0, 0.02, 0.2 or 2 μM of gefitinib for 6 hr and harvested in EBC buffer. Total cellular lysates were separated on SDS-PAGE, transferred to a membrane and blotted with (*a*) anti-phospho-AKT (Ser473) and (*b*) anti-phospho-Erk (p44/42) antibodies. The expression levels are shown in a graph.

require EGFR expression? Naruse *et al.*[32] suggested that the high sensitivity of K562/TPA to gefitinib is due to acquired EGFR expression. In their study autophosphorylation of EGFR in K562/TPA cells was inhibited by 0.01 μM gefitinib, and the IC_{50}-value of gefitinib in parental K562 cells, which do not express EGFR, was approximately 400-fold higher than that in the K562/TPA subline. Furthermore, most patients who responded to gefitinib therapy have *EGFR* mutation in lung tumor.[18,19] These findings suggest strongly that gefitinib exerts its antitumor effect through an action on EGFR. Our present study showed similar EGFR expression and autophosphorylation levels in PC-9 and PC-9/ZD cells. The inhibitory effect of gefitinib on phosphorylation of EGFR is different. PC-9/ZD did not show cross-resistance to the specific EGFR TK inhibitors RG-14620 and Lavendustin A in an MTT assay, nor did inhibit the phosphorylation of EGFR at the cellular level (data not shown). Paez *et al.*[18] reported that phosphorylation of EGFR in gefitinib-resistant cell lines was inhibited only when gefitinib was present at high concentration. These findings suggest that the difference in the inhibitory-effect on EGFR phosphorylation may determine the efficacy of the drug.

The inhibitory effect of gefitinib on EGFR phosphorylation is not significant in PC-9/ZD cells despite the absence of differences in the sequences of *EGFR*, *HER2*, and *HER3*. There are several possible explanations for the difference in inhibitory effect. First, the avidity of gefitinib for the ATP-binding site of EGFR may be decreased in PC-9/ZD cells due to a protein-protein interaction, *i.e.*, EGFR and a certain protein prevent gefitinib from binding to EGFR. Second, a change in the activity of specific protein-tyrosine kinase or phosphatase of EGFR in PC-9/ZD cells, especially after exposure to gefitinib, may result in resistance to inhibition of EGFR phosphorylation. The phosphorylation level is maintained in exquisite balance by the reciprocal activities of kinase and phosphatase,[33,34] and Wu reported that phosphatase plays a role in STI571-resistance.[35] Third, increased heterodimer formation by EGFR with other members of the HER family results in the limited inhibition. Heterodimer formation is increased in PC-9/ZD cells under basal conditions, and no increase in formation was observed after exposure to gefitinib, although marked heterodimer induction was observed in PC-9 cells. Calculations in *in vitro* studies have shown that the IC_{50}-value for inhibition of the tyrosine kinase activity of EGFR is 0.023–0.079 μM, whereas the IC_{50}-value for inhibition of HER2 is 100-fold higher.[36] We estimate that the inhibitory effect of gefitinib depends on the ratio of homodimer formation to heterodimer formation, and the heterodimer may be one of the routes of escape from the action of gefitinib.

Signal transduction by the HER family member is mediated by 2 major pathways, the MAPK signaling pathway and the AKT signaling pathway, which regulate cell proliferation and survival. Because phosphorylated AKT was inhibited completely by gefitinib in PC-9 cells, but inhibition of phosphorylated MAPK was not significant, inhibition of the AKT pathway may be more important to cell sensitivity than inhibition of MAPK. Moasser *et al.*[37] reported consistent results, showing that downregulation of AKT activity is predominantly seen in tumors that are sensitive to gefitinib. The phosphorylation of AKT and MAPK was not inhibited significantly by gefitinib in PC-9/ZD cells. This finding might be attributable to inactivation of Tyr 1068-GRB2-SOS-mediated signaling.

Based on the results of this comparative study, EGFR-GRB2-SOS complex formation, phosphorylation of Tyr1068, the ratio of the amount of homodimer formation to heterodimer formation, and the AKT signaling pathway are possible predictive biomarkers for gefitinib sensitivity. As a different approach, we are now looking for the genes associated with gefitinib resistance in PC-9/ZD cells compared to PC-9 cells by subtractive cloning.

Acknowledgements

'Iressa' is a trademark of the AstraZeneca group of companies.

References

1. Socinski MA. Addressing the optimal duration of therapy in advanced, metastatic non-small-cell lung cancer. In: Perry MC, eds. American Society of Clinical Oncology Educational Book. Alexandria: Lisa Greaves, 2003;144–52.
2. Nicholson RI, Gee JM, Harper ME. EGFR and cancer prognosis. Eur J Cancer 2001;37:S9–15.
3. Mendelsohn J, Baselga J. The EGF receptor family as targets for cancer therapy. Oncogene 2000;19:6550–65.
4. Salmon DS, Brandt R, Ciardiello F, Normanno N. Epidermal growth factor-related peptides and their receptors in human malignancies. Crit Rev Oncol Hematol 1995;19:182–232.
5. Fox SB, Smith K, Hollyer J, Greenall M, Hastrich D, Harris AL. The epidermal growth factor receptor as a prognostic marker: result of 370 patients and review of 3009 patients. Breast Cancer Res Treat 1994;29:41–99.
6. Dassonville O, Formento JL, Francoual M, Ramaioli A, Santini J, Schneider M, Demard F. Expression of epidermal growth factor receptor and survival in upper aerodigestive tract cancer. J Clin Oncol 1993;11:1873–8.
7. Sainsbury JR, Farndon JR, Needham GK, Malcolm AJ, Harris AL. Epidermal-growth-factor receptor status as predictor of early recurrence of and death from breast cancer. Lancet 1987;1:1398–402.
8. Scambia G, Benedetti-Panici P, Ferrandina G, Distefano M, Salerno G, Romanini ME, Fagotti A, Mancuso S. Epidermal growth factor, oestrogen and progesterone receptor expression in primary ovarian cancer: correlation with clinical outcome and response to chemotherapy. Br J Cancer 1995;72:361–6.
9. Veale D, Ashcroft T, Marsh C, Gibson GJ, Harris AL. Epidermal growth factor receptors in non-small cell lung cancer. Br J Cancer 1987;55:513–6.
10. Veale D, Kerr N, Gibson GJ, Kelly PJ, Harris AL. The relationship of quantitative epidermal growth factor receptor expression in non-small cell lung cancer to long term survival. Br J Cancer 1993;68:162–5.
11. Druker BJ, Talpaz M, Resta DJ, Peng B, Buchdunger E, Ford JM, Lydon NB, Kantarjian H, Capdeville R, Ohno-Jones S, Sawyers CL. Efficacy and safety of a specific inhibitor of the BCR-ABL tyrosine kinase in chronic myeloid leukemia. N Engl J Med 2001;344:1031–7.
12. Druker BJ, Sawyers CL, Kantarjian H, Resta DJ, Reese SF, Ford JM, Capdeville R, Talpaz M. Activity of a specific inhibitor of the BCR-ABL tyrosine kinase in the blast crisis of chronic myeloid leukemia and acute lymphoblastic leukemia with the Philadelphia chromosome. N Engl J Med 2001;344:1038–42.
13. Joensuu H, Roberts PJ, Sarlomo-Rikala M, Andersson LC, Tervahartiala P, Tuveson D, Silberman S, Capdeville R, Dimitrijevic S, Druker B, Demetri GD. Effect of the tyrosine kinase inhibitor STI571 in a patient with a metastatic gastrointestinal stromal tumor. N Engl J Med 2001;344:1052–6.
14. Fukuoka M, Yano S, Giaccone G, Tamura T, Nakagawa K, Douillard JY, Nishiwaki Y, Vansteenkiste J, Kudoh S, Rischin D, Eek R, Horai T, et al. Multi-institutional randomized phase II trial of gefitinib for previously treated patients with advanced non-small-cell lung cancer. J Clin Oncol 2003;21:2227–9.
15. Kris MG, Natale RB, Herbst RS, Lynch TJ Jr, Prager D, Belani CP, Schiller JH, Kelly K, Spiridonidis H, Sandler A, Albain KS, Cella D, et al. Efficacy of gefitinib, an inhibitor of the epidermal growth factor receptor tyrosine kinase, in symptomatic patients with non-small cell lung cancer: a randomized trial. JAMA 2003;290:2149–58.
16. Giaccone G, Herbst RS, Manegold C, Scagliotti G, Rosell R, Miller V, Natale RB, Schiller JH, Von Pawel J, Pluzanska A, Gatzemeier U, Grous J, *et al.* Gefitinib in combination with gemcitabine and cisplatin in advanced non-small-cell lung cancer: a phase III trial—INTACT 1. J Clin Oncol 2004;22: 777–84.
17. Miller VA, Johnson DH, Krug LM, Pizzo B, Tyson L, Perez W, Krozely P, Sandler A, Carbone D, Heelan RT, Kris MG, Smith R, et al. Pilot trial of the epidermal growth factor receptor tyrosine kinase inhibitor gefitinib plus carboplatin and paclitaxel in patients with stage IIIB or IV non-small-cell lung cancer. J Clin Oncol 2003;21: 2094–100.
18. Paez JG, Janne PA, Lee JC, Tracy S, Greulich H, Gabriel S, Herman P, Kaye FJ, Lindeman N, Boggon TJ, Naoki K, Sasaki H, et al. EGFR mutations in lung cancer: correlation with clinical response to gefitinib therapy. Science 2004;304:1497–500.
19. Lynch TJ, Bell DW, Sordella R, Gurubhagavatula S, Okimoto RA, Brannigan BW, Harris PL, Haserlat SM, Supko JG, Haluska FG, Louis DN, Christiani DC, et al. Activating mutations in the epidermal growth factor receptor underlying responsiveness of non-small-cell lung cancer to gefitinib. N Engl J Med 2004;350: 2191–3.
20. Pao W, Miller V, Zakowski M, Doherty J, Politi K, Sarkaria I, Singh B, Heelan R, Rusch V, Fulton L, Mardis E, Kupfer D, et al. EGF receptor gene mutations are common in lung cancers from "never smokers" and are associated with sensitivity of tumors to gefitinib and erlotinib. Proc Natl Acad Sci USA 2004; 101:13306–11.
21. Nomori H, Saijo N, Fujita J, Hyoi M, Sasaki Y, Shimizu E, Kanzawa F, Inomata M, Hoshi A. Detection of NK activity and antibody-dependent cellular cytotoxicity of lymphocytes by human tumor clonogenic assay—its correlation with the 51Cr-release assay. Int J Cancer 1985;35:449–55.
22. Mosmann T. Rapid colorimetric assay for cellular growth and survival: application to proliferation and cytotoxicity assays. J Immunol Meth 1983;65:55–63.
23. Arteaga CL, Ramsey TT, Shawver LK, Guyer CA. Unliganded epidermal growth factor receptor dimerization induced by direct interaction of quinazolines with ATP binding site. J Biol Chem 1998;273:18623–32.
24. Gorre ME, Mohammed M, Ellwood K, Hsu N, Paquette R, Rao PN, Sawyers CL. Clinical resistance to STI-571 cancer therapy caused by BCR-ABL gene mutation or amplification. Science 2001;293:876–80.
25. Von Bubnoff N. BCR-ABL gene mutation in relation to clinical resistance Lancet 2002;356:487–91.
26. McCormick F. New-age drug meets resistance. Nature 2001;412: 281–2.
27. Ricci C, Scappini B, Divoky V, Onida F, Verstovsek S, Kantarjian HM, Beran M. Mutation in the ATP binding pocket of the ABL kinase domain in and STI571-resistant BCR/ABL-positive cell line. Cancer Res 2002;62:5995–8.
28. Laffargue M, Raynal P, Yart A, Peres C, Wetzker R, Roche S, Payrastre B, Chap H. An epidermal growth factor receptor/Gab1 signaling pathway is required for activation of phosphoinositide 3-kinase by lysophosphatidic acid. J Biol Chem 1999;274:32835–41.
29. Rodriguez-Viciana P, Warne PH, Dhand R, Vanhaesebroeck B, Gout I, Fry MJ, Waterfield MD, Downward J. Phosphatidylinositol-3-OH kinase as a direct target of Ras. Nature 1994;370:527–32.
30. Kurata T, Tamura K, Kaneda H, Nogami T, Uejima H, Asai Go G, Nakagawa K, Fukuoka M. Effect of re-treatment with gefitinib ('Iressa', ZD1839) after acquisition of resistance. Ann Oncol 2004;15:173–4.
31. Yanase K, Tsukahara S, Asada S, Ishikawa E, Imai Y, Sugimoto Y. Gefitinib reverses breast cancer resistence protein-mediated drug resistence. Mol Cancer Ther 2004;3:1119–25.
32. Naruse I, Ohmori T, Ao Y, Fukumoto H, Kuroki T, Mori M, Saijo N, Nishio K. Antitumor activity of the selective epidermal growth factor receptor- tyrosine kinase inhibitor (EGFR-TKI) Iressatm (ZD1839) in a EGFR-expressing multidrug resistant cell line in vitro and in vivo. Int J Cancer 2002;98:310–5.
33. Reynolds AR, Tischer C, Verveer PJ, Rocks O, Bastiaens PIH. EGFR activation coupled to inhibition of tyrosine phosphatases causes lateral signal propagation. Nat Cell Biol 2003;5:447–53.
34. Haj FG, Markova B, Klaman LD, Bohmer FD, Neel BG. Regulation of receptor tyrosine kinase signaling by protein tyrosine phosphatase-1B. J Biol Chem 2003;278:739–44.
35. Wu JY, Talpaz M, Donato NJ. Tyrosine kinases and phosphatase play a role in STI571-mediate apoptosis of chronic myelogenous leukemia cells. Proc Am Assoc Cancer Res 2003;44(2nd ed.) 205:(Abstract 1016).
36. Wakeling AE, Guy SP, Woodburn JR, Ashton SE, Curry BJ, Barker AJ, Gibson KH. ZD1839 (Iressa): an orally active inhibitor of epidermal growth factor signaling with potential for cancer therapy. Cancer Res 2002;62:5749–54.
37. Moasser MM, Basso A, Averbuch SD, Rosen N. The tyrosine kinase inhibitor ZD1839 ("Iressa") inhibits HER2-driven signaling and suppresses the growth of HER2-overexpressing tumor cells. Cancer Res 2001;61:7184–8.

Development and biological analysis of peritoneal metastasis mouse models for human scirrhous stomach cancer

Kazuyoshi Yanagihara,[1,6] Misato Takigahira,[1] Hiromi Tanaka,[1] Teruo Komatsu,[1] Hisao Fukumoto,[5] Fumiaki Koizumi,[5] Kazuto Nishio,[2] Takahiro Ochiya,[3] Yoshinori Ino[4] and Setsuo Hirohashi[4]

[1]Central Animal Laboratory; [2]Pharmacology Division; [3]Section for Studies on Metastasis; [4]Pathology Division, National Cancer Center Research Institute; and [5]Shien-Lab Medical Oncology Department, National Cancer Center Hospital, 5-1-1 Tsukiji, Chuo-ku, Tokyo 104-0045, Japan

(Received February 23, 2005/Accepted March 26, 2005/Online publication June 15, 2005)

The number of published studies on peritoneal dissemination of scirrhous gastric carcinoma is very small as a result of the unavailability of highly reproducible animal models. Orthotopic implantation of HSC-44PE and HSC-58 (scirrhous gastric carcinoma-derived cell lines) cells into nude mice led to dissemination of the tumor cells to the greater omentum, mesenterium, peritoneum and so on, and caused ascites in a small number of animals. Cycles of isolation of the ascitic tumor cells and orthotopic inoculation of these cells were repeated in turn to animals. This was to isolate highly metastatic cell lines with a strong capability of inducing the formation of ascites (44As3 from HSC-44PE; 58As1 and 58As9 from HSC-58). All three cell lines induced tumor formation at the site of orthotopic injection, and caused fatal cancerous peritonitis and bloody ascites in 90–100% of the animals approximately 3–5 weeks after the inoculation. When the parent cells were implanted, the animals became moribund in approximately 12–18 weeks, however, none of the animals developed ascites. Complementary DNA microarray and immunohistochemical analyses revealed differences in the expression levels of genes coding for the matrix proteinase, cell adhesion, motility, angiogenesis and proliferation between the highly metastatic- and parent-cell lines. The usefulness of this model for the evaluation of drugs was assessed by analyzing the stability of the metastatic potential of the cells and the reproducibility. Animals intravenously treated with CPT-11 and GEM showed suppressed tumor growth and significantly prolonged survival. The metastatic cell lines and the *in vivo* model established in the present study are expected to serve as a model of cancerous peritonitis developing from primary lesions, and as a useful means of clarifying the pathophysiology of peritoneal dissemination of scirrhous gastric carcinoma and the development of drugs for its treatment. (*Cancer Sci* 2005; 96: 323–332)

Although therapeutic results for gastric cancer have improved recently, the prognosis of patients with scirrhous gastric carcinoma still remains very poor. Scirrhous gastric carcinoma (diffusely infiltrative carcinoma or Borrmann's type-IV carcinoma, or the linitis plastica-type carcinoma) is characterized macroscopically by rigid thickening of the involved region of the gastric wall, causing it to assume a plate-like appearance, rather than by a well-defined mass.[1] Histopathologically, scirrhous cancer cells do not form glands, but cause diffuse infiltration of a broad region of the gastric wall, resulting in fibrous-like thickening of the gastric wall.[2,3] Because of such pathological features, early clinical diagnosis of scirrhous gastric carcinoma is difficult. By the time the diagnosis is made, peritoneal dissemination or distant metastasis to lymph nodes has already occurred in many cases. Peritoneal dissemination occurs frequently even after radical surgery, and is the cause of death in many patients.[4,5] Thus, peritoneal dissemination, a frequent form of recurrence and metastasis of scirrhous gastric carcinoma, serves as a major factor determining the prognosis of patients with scirrhous gastric carcinoma. To date, however, the mechanism of peritoneal dissemination in this type of cancer has not yet been fully elucidated.

Several theories have been proposed to explain the mechanism of peritoneal dissemination in human gastric cancer; it has been suggested that the cancer cells are detached from the primary lesions and freed into the peritoneal cavity, to colonize the peritoneum and induce cancerous peritonitis. However, most of the proposed theories remain speculations, and are seldom based on adequate evidence.[6–8] It cannot be overemphasized therefore that animal models of this condition are urgently needed to pursue studies on its pathophysiology. Some investigators have reported on a model of this condition established by direct inoculation of cultured gastric cancer cells into the peritoneal cavity.[9,10] It is difficult, however, to view this model as faithfully reflecting the characteristics of cancerous peritonitis observed in clinical cases. In the past, it was considered difficult to reliably establish a model of peritoneal dissemination developing from the primary lesions. Under these circumstances, we established seven cultured cell lines derived from human scirrhous gastric carcinoma and analyzed their characteristics.[11–14] Of these cell lines, the HSC-44PE and HSC-58 cells were found to show spontaneous metastasis to lymph nodes and lungs following s.c. implantation in nude mice.[14] Then, to isolate cell lines with a high metastatic potential, we performed repetitive s.c. inoculation of these cell lines and isolated sublines that tended to metastasize to lymph nodes. When these sublines were implanted orthotopically, a small number of animals showed massive bloody ascites. This phenomenon resembled the cancerous peritonitis seen in clinical cases and suggested a high possibility of establishing a reproducible mouse model of peritoneal dissemination.

In the present paper, we shall report on an analysis of the characteristics of tumor cell lines that often cause ascites (cell lines with a high potential for peritoneal dissemination) isolated by repeated orthotopic implantation of HSC-44PE and HSC-58 cells. The paper will also describe the results of cDNA microarray and immunohistochemical analyses of these cell lines as the first step towards clarifying the molecular mechanism of development of peritoneal metastasis in gastric cancer. In addition, the usefulness of these cell lines as a model for drug evaluation will also be discussed.

[6]To whom correspondence should be addressed. E-mail: kyanagih@gan2.res.ncc.go.jp
Abbreviations: cDNA, complementary DNA; CPT-11, camptothecin; GEM, gemcitabine; s.c., subcutaneously; i.p., intraperitoneally; i.v., intravenously.

 doi: 10.1111/j.1349-7006.2005.00054.x

Materials and Methods

Cell lines and culture. HSC-39, HSC-44PE and HSC-58 and cell lines established from human scirrhous gastric carcinomas have been reported previously.[11,14] The cell lines were maintained in RPMI1640 medium (Immuno-Biological Laboratories (IBL), Takasaki, Japan) supplemented with 10% FCS (Sigma Chemical, St. Louis, MO, USA), 100 IU/mL penicillin G sodium and 100 μg/mL streptomycin sulfate (IBL) in a 5% CO_2 and 95% air atmosphere at 37°C. The cells were passaged and expanded by trypsinization (0.05% trypsin and 0.02% EDTA; IBL), followed by replating every 5–7 days. All the cell lines were routinely tested for Mycoplasma by the Central Institute for Experimental Animals (Kawasaki, Japan), and no contamination was detected. For injection into mice, cells in log-phase growth were harvested by trypsinization and washed with serum-free RPMI1640 medium.

Animal experimentation. The animal experimental protocols were approved by the Committee for Ethics of Animal Experimentation, and the experiments were conducted in accordance with the Guidelines for Animal Experiments in the National Cancer Center. The mice were purchased from CLEA Japan (Tokyo, Japan) and maintained under specific pathogen-free conditions. They were provided with sterile food and water and housed in cages. The ambient light was controlled to provide regular 12-h light and 12-h darkness cycles.

Establishment of cell lines with a strong potential for inducing the formation of peritoneal metastasis. HSC-44PE and HSC-58 cell lines were inoculated by the orthotopic implantation technique into BALB/c nude mice. At appropriate intervals, or when moribund, the mice were sacrificed and the ascitic tumor cells were harvested aseptically. The cell suspensions were then cultured *in vitro*. The same procedure was repeated using both cell lines, and cell lines with a high potential for inducing the formation of peritoneal metastasis were established after 12 cycles of stepwise selection. Each resultant cell line after *in vitro* passages 5–10 was used for experiments.

Orthotopic implantation. Six-week-old female BALB/c nude mice were anesthetized by i.p. injection of 2.2.2-tribromoethanol (Aldrich Chemical, Milwaukee, WI, USA) at the dose of 0.28 mg/g bodyweight. Then, after making a small median abdominal incision in the mice under anesthesia, 2×10^6 cells in 0.05-mL volume of RPMI medium were inoculated into the middle wall of the greater curvature of the glandular portion of the stomach using a 30-gauge needle (Nipro, Tokyo, Japan). The stomach was then returned into the peritoneal cavity, and the abdominal wall and skin were closed with an AUTOCLIP applier (Becton-Dickinson, Sparks, MD, USA). The mice were killed 200 days after the tumor cell inoculation or when moribund, and peritoneal dissemination was evaluated by counting the number of tumor nodules in the mesenterium. The body organs were examined for metastasis, and various tissues were processed for histological examination.

Evaluation of the growth rate and metastatic potential of the cell lines. The tumorigenicity and spontaneous-metastatic potential of the cell lines were tested by s.c. injection of $0.5–1 \times 10^7$ cells suspended in 0.2 mL of RPMI1640 medium into 6-week-old female BALB/c nude mice. All the mice were numbered, housed separately, and examined twice weekly for tumor development. The tumor mass was measured in two dimensions with calipers, and the tumor volume was calculated according to the equation $(l \times w^2)/2$ (l = length, w = width). At appropriate intervals or when moribund, the mice were killed, and various organs and tissues were examined for metastasis and processed for histological examination as described.[11]

Therapeutic studies with CPT-11 and GEM. Orthotopic implantation of 2×10^6 44As3 or 58As1 cells was conducted in 6-week-old female BALB/c mice (Day 0). The experimental mice were divided into a control group that received vehicle alone (saline), and experimental groups that received i.v. inoculation of different doses of the drugs (50–200 mg/kg/mouse). On Days 3, 7 and 11, tumor-bearing mice received an i.v. injection of 7-Ethyl-10-[4-(1-piperidino)-1-piperidino] carboxycamptothecin (CPT-11). CPT-11 was purchased from Yakult Honsha (Tokyo, Japan) and dissolved in saline before being injected i.v. Gemcitabine (gemcitabine hydrochloride), chemically characterized as (+)-2′-deoxy-2′, 2′-difluorocytidine monohydrochloride, was purchased from Eli Lilly Japan (Kobe, Japan). The mice were administered i.v. inoculations of GEM on days 3, 7, 10, 14, 17, and 21. Seven mice from each group were killed when moribund, or on Day 70.

Statistical analysis. All the data were expressed as the mean ± SE, and analyzed using the unpaired t-test and a *P*-value of less than 0.001 was considered to denote statistical significance.

RT-PCR analysis. Total RNA was extracted using the ISOGEN/ISOGEN-LS Poly (A) + Isolation Pack (Nippon Gene, Tokyo, Japan), in accordance with the supplier's protocol. After reverse transcription using 1 μg total RNA with an oligo (dT) primer, the whole mixture was used for PCR detecting human and murine β actin. The primers used were as follows; human β actin forward primer, GGAAATCGTGCGTGACATT; reverse primer, CATCTGCTGGAAGGTGGACAG; murine β actin forward primer, GAAATCGTGCGTGACATCAAA; reverse primer, TACTGGTGCTAGGAGCCA. PCR was performed using an RNA PCR kit (Applied Biosystems, Foster City, CA, USA), under the following conditions; initial denaturation at 95°C for 2 min, 35 cycles of amplification (denaturation at 95°C for 60 s and annealing at 60°C for 60 s), and extension at 72°C for 7 min. The PCR products were electrophoresed on 2% agarose gel, and stained with ethidium bromide.

Gene expression profiling by cDNA microarray analysis. 5 μg total RNA was amplified using an *in vitro* transcription reaction.[15] The amplified RNA (6 μg) was reverse-transcribed using random hexamers and aminoallyl-dUTP. The synthesized cDNA was labeled by allowing it to react with a dye (NHS-ester Cy3 or Cy5, Amersham Biosciences, Buckinghamshire, UK).[16] The labeled cDNA was applied to the DNA microarray (Human IA; Agilent Technologies, Palo Alto, CA, USA) and hybridized at 65°C for 17 h. After washing, the microarray was scanned on a scanner (Agilent, G2565BA) and the image was analyzed using a Feature Extraction software (Agilent). The signal intensity of each spot was calibrated by subtraction from the intensity of the negative control. Global normalization methods were used for identification of the differentially expressed genes in each microarray experiment.

Immunohistochemical Analysis. Mouse antibodies against human Cathepsin L (C2970) and MMP-1 (M6427: Sigma-Aldrich, St. Louis, MO, USA), human VEGF (JH121: Laboratory Vision, Fremont, CA, USA), human EGER (31G7: Zymed Laboratory, San Francisco, CA, USA) and human Smad4 (B-8; Santa Cruz Biotechnology, Santa Cruz, CA, USA) were used for this study. The other antibodies used have been described in a previous study.[14] Immunohistochemical staining was carried out as described previously.[8] The staining was repeated to check for possible technical errors, but the results were consistent. Scores for the expression of various genes were assigned semiquantitatively according to the percentage of the cells stained and the staining intensity.

Results

Establishment of the highly metastatic cell lines. Following s.c. inoculation, 20–40% of the HSC-44PE and HSC-58 cells (cultured scirrhous gastric carcinoma cells) metastasized spontaneously to the regional lymph nodes and lungs. When the subclones isolated by repeated s.c. injection of these cells were implanted orthotopically, they spread to the greater omentum,

 doi: 10.1111/j.1349-7006.2005.00054.x

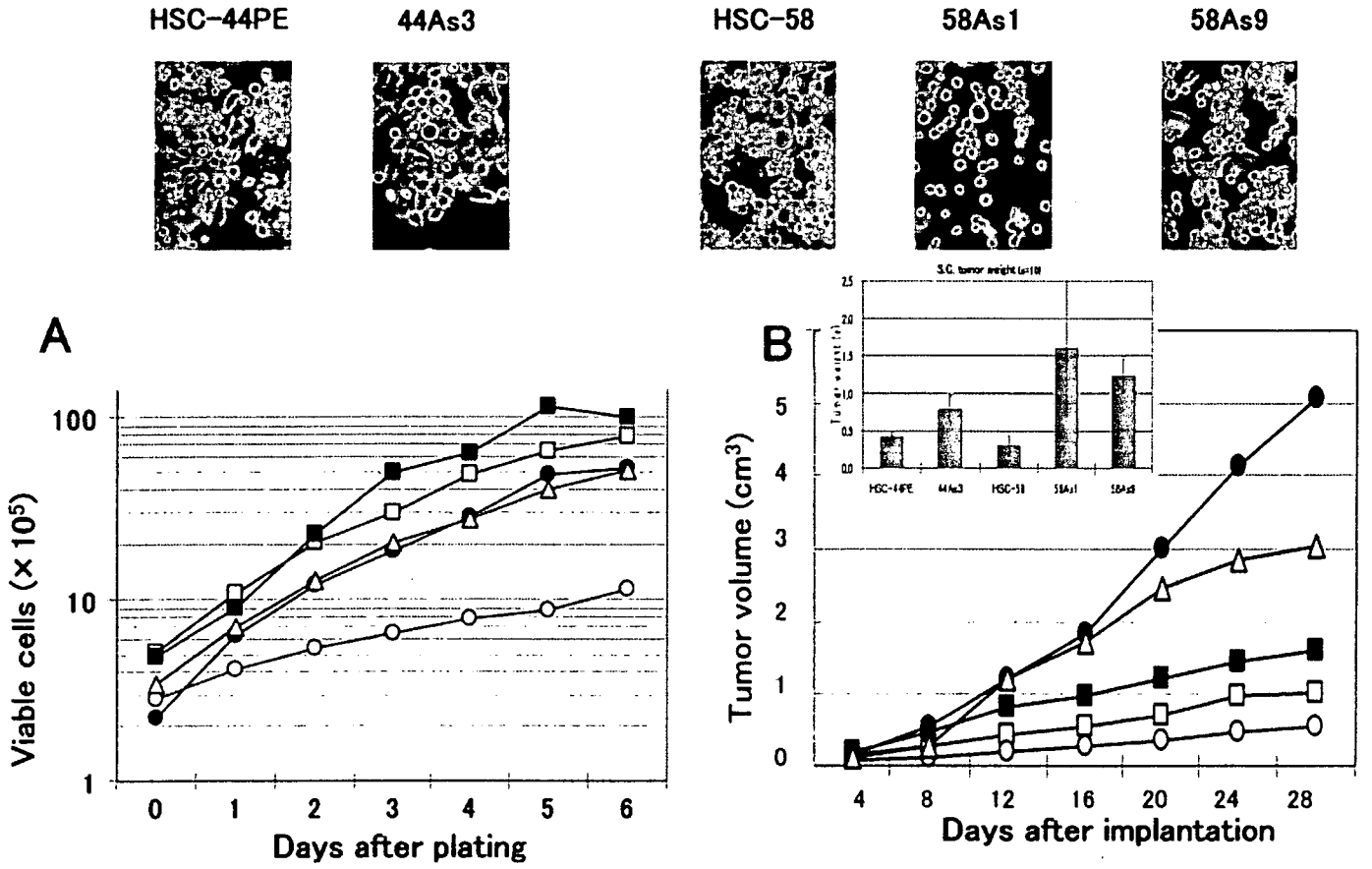

Fig. 1. Phase-contrast micrographs and the growth properties of the sublines showing a high metastatic potential and their parent cell lines. Original magnification, ×200. (A), Growth curves of the cells *in vitro*. Cells were seeded at a density of 1×10^5 cells/well in 6-well plates (Falcon, Lincoln Park, NJ, USA), and the cell numbers were determined daily. The results of a representative experiment are given and the points indicate the average of the results in 3 wells in which the cell numbers varied by 10%. (B), Growth curves of the cells *in vivo*. Tumor volume was measured at predetermined time intervals described in 'Materials and Methods.' HSC-44PE (□), 44As3 (■), HSC-58 (○), 58As1 (●), and 58As9 (△) cell lines were used. Similar results were obtained in a second experiment conducted independently.

mesenterium and so on, and caused the formation of bloody ascites in a small number of animals.[14] Following this result, we incubated the cancer cells isolated from the ascitic fluid of mice, which developed cancerous peritonitis 3–6 months following the orthotopic implantation of HSC-44PE and HSC-58 cells, and attempted orthotopic injection of the incubated cells. This sequence of manipulations was repeated for 12 cycles in an attempt to reliably isolate cell lines that would have higher potentials of undergoing metastasis (in the form of dissemination) over short periods of time. We first obtained a cell line (44As3) from HSC-44PE cells that possessed a high metastatic potential, with a strong capability of inducing ascites. The 44As3 cells resembled the parent HSC-44PE cells in their morphological characteristics. While most cells of this subline exhibited high adhesivity, a small number of spherical cells remained floating and showed proliferative activity. Occasional signet ring cells were also observed (Fig. 1). Although the proliferative potential of the 44As3 cells did not differ greatly from that of the parent cell line *in vitro* (Fig. 1A), the former induced more rapid s.c. tumor formation than the latter (Fig. 1B).

Two highly metastatic cell lines (58As1 and 58As9) were also established from the HSC-58 cells. The 58As1 cells assumed the form of aggregates of spherical cells with low adhesive capacity, which remained floating and showed proliferative activity. In contrast, 58As9 cells often exhibited high adhesivity, resembling the parent cell line, HSC-58, in this characteristic (Fig. 1). Both 58As1 and 58As9 cells exhibited higher proliferative potential *in vitro* than the parent HSC-58 cells (Fig. 1A), and the tumor-forming capability following s.c. injection of these subclones differed markedly from that of the parent cell line; the 58As1 cells, in particular, showed a markedly higher tumor-forming capability (Fig. 1B).

Comparison of the highly metastatic cell lines and the parent cell lines *in vivo*. Table 1 shows the metastatic behavior and the survival days of animals following orthotopic injection of the tumor cells. Orthotopic implantation of 44As3 cells resulted in the formation of bloody ascites approximately 20 days later, and some mice became moribund (Fig. 2D). Dissemination was most often seen to the greater omentum, mesenterium, parietal peritoneum, diaphragm, and so on. Metastasis to the regional lymph nodes and liver was also frequently seen (Table 1). Micrometastasis was observed in the pancreas (also in the lungs, although rarely). The percentage of parent HSC-44PE cells that survived at the site of implantation was 68%. Inoculation of HSC-44PE cells resulted in the animals becoming moribund approximately 85 days after the implantation, but none of the animals developed ascites (Table 1, Fig. 2D).

When 58As1 or 58As9 cells were implanted orthotopically, bloody ascites began to form approximately 3 weeks after the inoculation, accompanied by tumor dissemination to the greater omentum, mesenterium, parietal peritoneum, diaphragm and so on, and the animals died soon thereafter (Table 1, Fig. 2A–C). Lymph node metastasis was observed in all the animals; metastasis to the liver was also noted. Micrometastases were seen in the pancreas and the lungs. Implantation of 58As1 cells was followed by the development of micrometastases in the

Table 1. Metastasis and peritoneal dissemination after orthotopic inoculation of human gastric cancer cell lines and sublines[†]

Cell line	Survival days	Tumor formation	Ascites	Lymph node	Lung[‡]	Liver	Pancreas[‡]	Kidney[‡]	Disseminated Metastasis			
									Omentum	Mesenterium	Parietal peritoneum	Diaphragm
HSC-44PE	131 ± 44 (85–200)	13/19 (68%)	0/13 (0%)	5/13	0/13	0/13	0/13	0/3	4/13	3/13	2/13	0/13
44As3	33 ± 11 (20–62)	21/21 (100%)	19/21 (90%)	21/21	2/21	19/21	10/21	0/21	21/21	21/21	20/21	14/21
HSC-58	85 ± 16 (68–123)	16/20 (80%)	1/16 (6%)	5/16	1/16	3/16	1/16	0/16	6/16	3/16	3/16	0/16
58As1	32 ± 5 (23–42)	21/21 (100%)	20/21 (95%)	21/21	6/21	19/21	7/21	4/21	21/21	21/21	21/21	13/21
58As9	45 ± 13 (22–68)	14/14 (100%)	14/14 (100%)	14/14	2/14	7/14	1/14	0/14	14/14	10/14	11/14	8/14

[†]Mice were killed at 200 days after the orthotopic implantation. Data are shown as the number of mice bearing metastasis at the site/total number of mice bearing tumor. [‡]Micrometastasis.

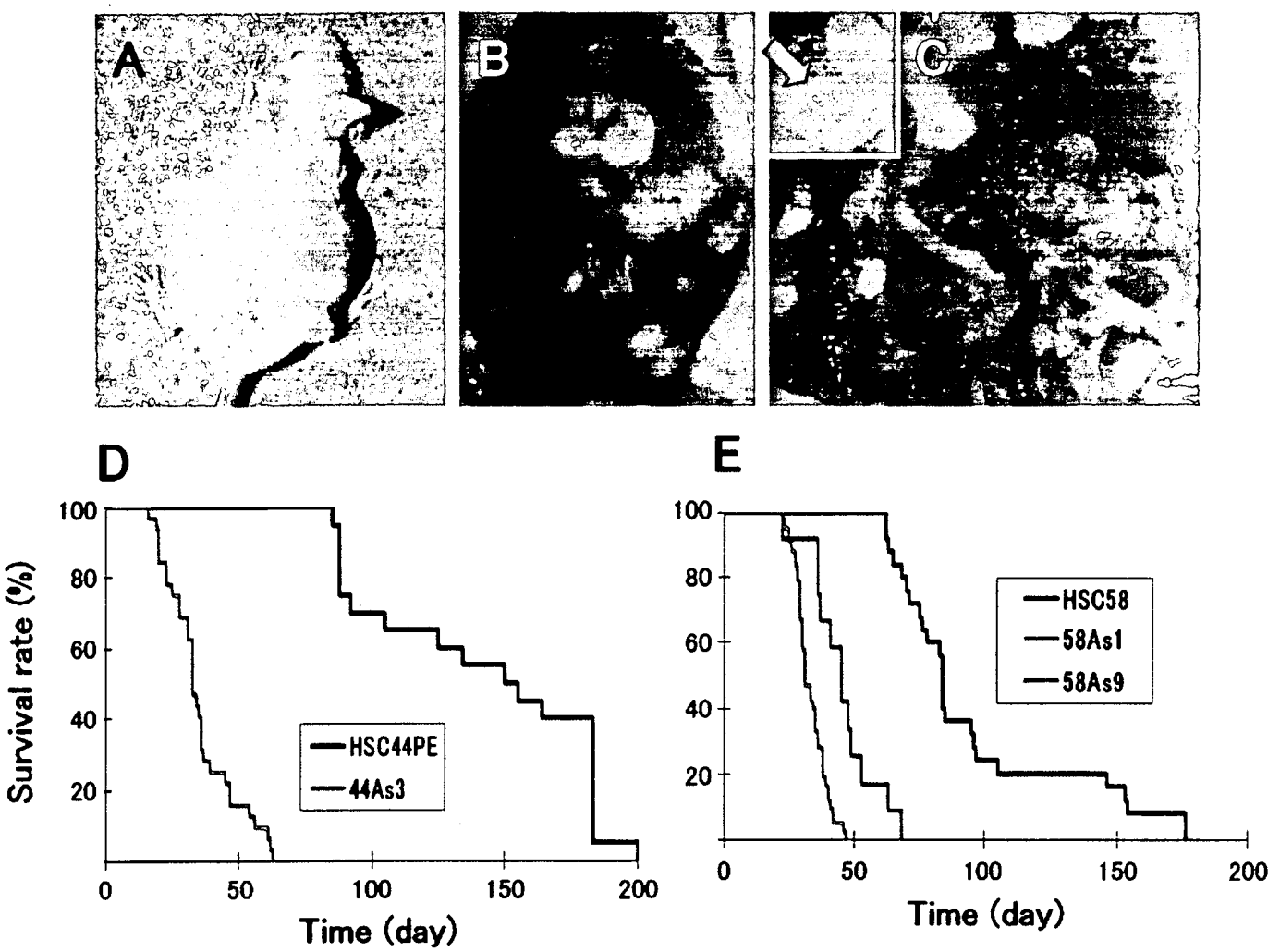

Fig. 2. Macroscopic appearance of the peritoneal disseminations, and survival of nude mice after orthotopic implantation of the cell lines. (A,B), Carcinomatous peritonitis was observed 4 weeks after orthotopic implantation of 58As1 cells. Abdominal distension because of bloody ascites was evident. (C), Peritoneal dissemination was recognized from the innumerable whitish nodules visualized in the abdominal cavity, mesenterium, omentum, parietal peritoneum and diaphragm. Orthotopic implantation of 58As1 cells in the stomach of nude mice was followed by tumor formation 3 weeks later (green arrow, inset). (D), Survival of 44As3-, and HSC-44PE-tumor-bearing mice ($n = 15$; $P < 0.001$). (E), Survival of 58As1-, 58As9-, and HSC-58-tumor-bearing mice ($n = 20$; $P < 0.001$). The experiments were repeated thrice and yielded similar results each time.

 doi: 10.1111/j.1349-7006.2005.00054.x

Table 2. Genes that show differential expression levels in 44As3 cells as compared with those in HSC-44PE cells

Ratio	Symbol	Gene name	Function and description
Upregulated gene			
29.63	*MMP1*	Matrix metalloproteinase 1	Proteolysis and peptidolysis, collagenase
11.25	*LOC57402*		Cell signaling
9.68	*I_1109564*	H19	Unknown function
4.92	*LGALS1*	Lectin, galactoside-binding, galectin 1	Apoptosis, cell adhesion
4.84	*I_930461*	Tropomyosin 2 (beta)	Contractile proteins
4.47	*AGR2*	Anterior gradient 2 homolog (Xenepus laevis)	Oncogenesis
4.40	*BOK*	BCL2-related ovarian killer	Induction of apoptosis
4.03	*NAP1L4*	Nucleosome assembly protein 1-like 4	Nucleosome assembly
3.99	*TNC*	Tenascin C (hexabrachion)	Binding, cell adhesion
3.98	*HSPB1*	Heat shock 27 kDa protein 1	Regulation of translational initiation
3.95	*HGD*	Homogentisate 1,2-dioxygenase	Tyrosine catabolism, phenylalanine catabolism
3.83	*PIGPC1*		Plasma membrane protein actvated by p53, cell death
3.52	*PIASY*		Apoptosis
3.48	*SYP*	Synaptophysin	Regulating neurotransmitter release
3.38	*RPS12*		Ribosomal protein S12
3.36	*CTSL*	Cathepsin L	Associated with highly invasive tumors
3.35	*HSPC018*		Unknown function
3.23	*INSIG1*	Insulin induced gene 1	Metabolism, cell proliferation
3.20	*I_962761*	Insulin induced gene 1	Metabolism, cell proliferation
3.17	*I_963048*		Immunity
Downregulated gene			
0.14	*THBS1*	Thrombospondin 1	Endopeptidase inhibitor, signal transducer, cell adhesion
0.34	*PRG1*	Proteoglycan 1, secretory granule	Proteoglycan
0.41	*CUL4B*	Cullin 4B	Cell cycle
0.41	*MCM3*	MCM3	Adenosinetriphosphatase, DNA binding
0.42	*NFE2L3*	Nuclear factor (erythroid-derived 2)-like 3	Transcription coactivator, transcription factor
0.43	*THBS4*	Thrombospondin 4	Heparin binding, calcium ion binding, cell adhesion
0.45	*CD59*	CD59 antigen p18–20	Lymphocyte antigen, defense response, signal transduction
0.46	*VBP1*	von Hippel-Lindau binding protein 1	Protein binding
0.46	*LOC51659*		Unkown function
0.47	*PODXL*		Lymphocyte adhesin and homing
0.47	*H2BFB*		H2B histon family member B
0.47	*ZNF195*	Zinc finger protein 195	
0.47	*MCT-1*		Cyclin, cell cycle
0.48	*CD44*	CD44 antigen	Transmembrane glycoprotein, extracellular matrix attachment
0.48	*NDUFA1*	NADH dehydrogenase (ubiquinone)	Energy pathways

kidney also. Although only rarely, pleural effusion and ovarian micrometastases were also noted (data not shown). Orthotopic injection of the parent cell line (HSC-58), however, resulted in the mice becoming moribund approximately 68 days after the implantation (Table 1, Fig. 2E). When the dead animals were autopsied, mild peritoneal dissemination was noted, but ascites were observed in only a very small number of animals (Table 1).

Comparison of gene expression between the highly metastatic- and the parent cell lines. The parent cell lines with a low potential for peritoneal dissemination were compared with the highly metastatic cell lines, using a cDNA microarray (approximately 30 000 genes; Agilent). The differences in the gene expression levels between the two types of cell lines were assessed by measuring the ratios of their expression. The ratio was rated as significant when it was over 2:1. The first 15 genes ranked in terms of this ratio are shown in Tables 2 and 3. When the highly metastatic cell line 44As3 was compared with its parent cell line HSC-44PE, the expression of 89 genes, such as that of MMP1 and cathepsin L, was more intense and that of 19 genes; for example, thrombospondin 1 was less intense in the 44As3 cells in comparison to the parent cell line (Table 2). Table 2 shows the results of a similar comparison of 58As1 and 58As9 cells (highly metastatic cell lines showing a marked increase of proliferative potential) with the parent cell line, HSC-58. Compared to that in the parent cell line, 58As1 cells showed more intense expression of 40 and less intense expression of 20 of the genes examined, while 58As9 cells showed more intense expression of 36 and less intense expression of 32 of the genes examined. In addition to the MMP1 and cathepsin L genes, genes encoding molecules associated with cell adhesion, motility, proliferation, apoptosis, metabolic enzymes and so on, also showed altered expression.

Then, the expression levels of MMP1 and cathepsin L were confirmed at the protein level and compared with the expression levels of known metastasis-associated genes (Table 4). Weak MMP1 protein expression was seen in 44As3 cells as well as 58As9 cells. The cathepsin L gene was expressed in HSC-44PE cells, but even stronger expression was observed in the 44As3 cells (Fig. 3A,B). Intense expression of this gene was also seen in the metastatic cell line, 58As1 (Fig. 3C). Moderate expression of the cathepsin L gene was observed in 58As9 cells, whereas expression of this gene was totally absent in the parent cell line (Fig. 3D). Molecules whose expression levels differed markedly between the parent cell line and the 58As1 or 58As9 cells were dysadherin, CD44, integrin β4, EGFR (Fig. 3E,F), HGF, and VEGF (Fig. 3G,H). While dysadherin was not expressed in the HSC-58 cells, it was expressed intensely in all the highly metastatic subclones (Fig. 3I,J). Intense expression of nm23

Table 3. Genes that show differential expression levels in 58As1 and 58As9 compared with that in HSC-58 cells

Ratio	Symbol	Gene name	Function and description
Upregulated genes 58As1			
19.41	*ADH1C*	Alcohol dehydrogenase 1C, gamma polypeptide	Zinc ion binding, electron transporter, metabolism
18.59	*ADH1B*	Alcohol dehydrogenase IB, beta polypeptide	Zinc ion binding, electron transporter, metabolism
17.70	*FABP1*	Fatty acid binding protein 1, liver	Lipid transporter, fatty acid metabolism, cell signaling
15.21	*ADH1A*	Alcohol dehydrogenase 1A, alpha polypeptide	Zinc ion binding, electron transporter, metabolism
14.15	*PLAT*	Plasminogen activator, tissue	Proteolysis and peptidolysis, blood coagulation
11.01	*MTP*	Microsomal triglyceride transfer protein subunit precursor	Lipid metabolism, Small molecule-binding protein
10.47	*AKR1C2*	Aldo-keto reductase family 1, member C2	Bile acid electron transporter, metabolism
4.71	*CYP1B1*	Cytochrome P450, family 1, subfamily B, polypeptide 1	Cytochrome P450, electron transporter, morphogenesis
4.67	*AKR1C3*	Aldo-keto reductase family 1, member C3	Electron transporter, metabolism, cell proliferation
4.04	*PON2*	Paraoxonase 2	Arylesterase
4.01	*RDHL*		NADP-dependent retinol dehydrogenase/reductase
3.73	*SERPINE2*	Serine proteinase inhibitor, clade E, member 2	Serpin, development
3.60	*PPP1R14A*	Protein phosphatase 1, regulatory subunit 14A	
3.54	*TGFBI*	Transforming growth factor, beta-induced, 68 kDa	Integrin binding, tumor suppressor, cell adhesion
3.45	*PROCR*	Protein C receptor, endothelial (EPCR)	Receptor, inflammatory response
Upregulated genes 58As9			
7.03	*AKR1C2*	Aldo-keto reductase family 1, member C2	Bile acid transporter, binding, electron transporter
6.08	*I_1109564*	H19, imprinted maternally expressed untranslated mRNA	Unknown function
5.95	*MKNK2*	MAP kinase-interacting serine/threonine kinase 2	Phosphorylation, signal transduction
4.10	*APOC1*	Apolipoprotein C-I	Lipid metabolism
4.07	*FLJ21841*		Unknown function
4.02	*SERPINE2*	Serine proteinase inhibitor, clade E, member 2	Serpin, development
3.77	*CTSL*	Cathepsin L	Cathepsin L, associated with highly invasive tumors
3.28	*AKR1C3*	Aldo-keto reductase family 1, member C3	Electron transporter, metabolism, cell proliferation
3.11	*SIAT8B*	Sialyltransferase 8B (alpha-2, 8-sialyltransferase)	Metabolism, embryogenesis and morphogenesis
3.01	*FKBP1B*	FK506 binding protein 1B	Popeptidylprolyl isomerase
2.82	*KIAA1247*		Member of the sulftase family
2.80	*I_1000731*	GRB2-associated binding protein 2	Protein-protein and protein–lipid interactions
2.77	*STMN3*	Stathmin-like 3	Neurogenesis, SCG10 like-protein, tumor progression
2.75	*ANK3*	Ankyrin 3, node of Ranvier (ankyrin G)	Cytoskeletal anchoring, vesicle transport
2.74	*CEBPE*	CCAAT/enhancer binding protein (C/EBP), epsilon	Transcription activating factor, defense response
Downregulation 58As1			
0.11	*LAMR1*	Laminin receptor 1	Signal transduction, cell adhesion, invasive growth
0.13	*S100A4*	S100 calcium binding protein A4	Calcium ion binding, invasive growth
0.15	*RARRES1*	Retinoic acid receptor responder	Negative regulation of cell proliferation
0.15	*HLA-DQB1*	HLA complex, class II, DQ beta 1 precursor	Immune response
0.15	*KLK6*	Kallikrein 6 (neurosin, zyme)	Serine-type peptidase, pathogenesis
0.16	*TM4SF4*	Transmembrane 4 superfamily member 4	Negative regulation of cell proliferation, glycosylation
0.16	*HLA-DRA*	Major histocompatibility complex, class II, DR alpha	Immune response
0.17	*CTNNB1*	Catenin (cadherin-associated pritein), beta 1, 88 kDa	Tumor suppressor, cell adhesion, transcription
0.19	*HLA-DRB3*	Major histocompatibility complex, class II, DR beta 3	Immune response
0.20	*SAT*	Spermidine/spermine N1-acetyltransferase	Diamine N-acetyltransferase, modulates tumorigenicity
0.20	*HLA-DRB5*	Major histocompatibility complex, class II, DR beta 5	Immune response
0.20	*I_966873*		Strong similarity to human HLA-DRB1
0.21	*FOS*	v-fos FBJ murine osteosarcoma viral oncogene homolog	Transcription, methylation, cell growth, oncogenesis
0.21	*I_965396*		Unknown, high similarity to charcterized human AG2
0.22	*CEACAM6*	Carcinoembryonic antigen-related cell adhesion molecule 6	Signal transduction, cell-cell signaling
Downregulation 58As9			
0.06	*CEACAM8*	Carcinoembryonic antigen-related cell adhesion molecule 8	Tumor antigen, immune response, cell adhesion
0.07	*TM4SF3*	Transmembrane 4 superfamily member 3	Signal transducer, tumor antigen, pathogenesis
0.07	*LAMR1*	Laminin receptor 1 (ribosomal protein SA, 67 kDa)	Signal transduction, cell adhesion, invasive growth
0.09	*CEACAM6*	Carcinoembryonic antigen-related cell adhesion molecule 6	Signal transduction, cell-cell signaling, cell adhesion
0.12	*CTNNB1*	Catenin (cadherin-associated pritein), beta 1, 88 kDa	Tumor suppressor, cell adhesion, oncogenesis
0.12	*KRT19*	Keratin 19	Structural constituent of cytoskeleton, differentiation
0.13	*KRTHA3A*	Keratin, hair, acidic, 3 A	Cell shape and cell size control
0.13	*CEACAM3*	Carcinoembryonic antigen-related cell adhesion molecule 3	Tumor antigen, immune response, cell adhesion
0.14	*I_966690*		Strong similarity to human HLA-DRB4
0.17	*S100A4*	S100 calcium binding protein A4	Calcium ion binding, invasive growth
0.20	*FOS*	v-fos FBJ murine osteosarcoma viral oncogene homolog	Transcription, methylation, cell growth, oncogenesis
0.22	*DAF*	Decay accelerating factor for complement (CD55)	Decay accelerating factor
0.23	*MYC*	v-myc myelocytomatosis viral oncogene homolog (avian)	Transcription factor, cell cycle, pathogenesis
0.24	*CRIP1*	Cysteine-rich protein 1 (intestinal)	Zinc ion binding, cell proliferation
0.24	*KRTHB6*	Keratin, hair, basic, 6	Monilethrix

 doi: 10.1111/j.1349-7006.2005.00054.x

Table 4. Expression of metastasis-related genes in the highly metastatic and the parent gastric cancer cell lines

Cell line	MMP-1	Cathepsin L	Cell adhesion					Oncogenes					Angiogenesis				nm23	Smad4
			CD44	E-cadherin	Dysadherin	β-catenin	Integrin α6β4	EGFR	c-erb-B-2	cript	c-met	HGF	bFGF	VEGF	IL-6	IL-8		
44As3	+	++	++a	++	++	++	—	++	–	+	+	–	–	+	–	–	++	–
HSC-44PE	–	+	++a	++	++	++	–++	++	–	+	+	+	–	+	–	–	–	–
58As1	–	++	++	–	++	++	–++	+	–	+	++a	++	+	++	–	–	++	–
58As9	+	+	++	–	++	+	–+	++	–	+	++a	+	+	++	–	–	+	–
HSC-58	–	–	+	–	–	++	—	–	–	+	++a	–	+	–	–	–	–	–

Immunohistochemical staining was carried out as described in a previous study.[8] ++, Moderate or strong staining intensity, or staining of > 75% of the cells; +, weak staining intensity, or staining of < 25% of the cells; –, negative staining, or staining of < 1% of the cells. a, gene amplification.

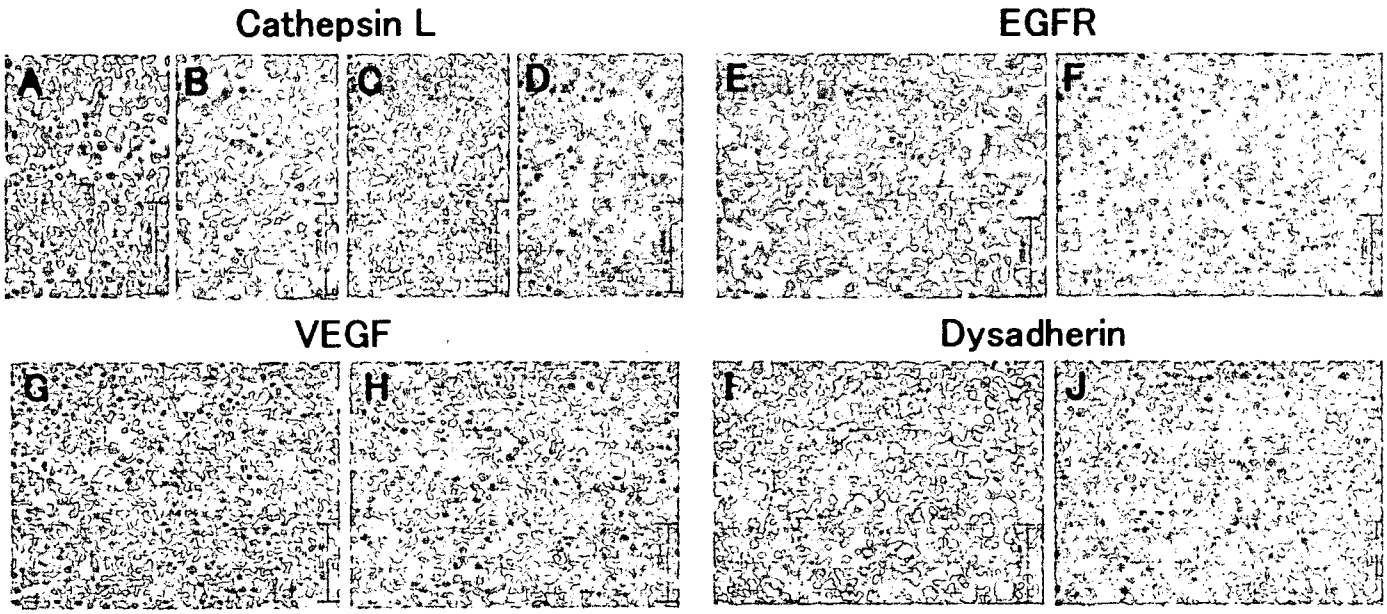

Fig. 3. Immunohistochemical analyses of Cathepsin L, EGFR, VEGF and Dysadherin in the highly metastatic and the parent cell lines. The metastatic 44As3 (A) and 58As1 (C) expressed strongly detectable cathepsin L in the cytoplasm. Immunoreactivity for cathepsin L observed weakly at the cytoplasm in HSC-44PE (B), but immunoreactivity completely absent from HSC-58 (D). (E), Expression of EGER is observed in the membranes of the 58As1 subclone. (F), Immunoreactivity for EGER was completely absent from HSC-58 cells. (G), Expression of VEGF is observed in the cytoplasm of the 58As9 cells, but immunoreactivity absent from HSC-58 (H). (I), Expression of dysadherin is observed at the cell-cell boundaries in 58As9 subclone. (J), Immunoreactivity for dysadherin was completely absent from HSC-58 cells.

was also observed in highly metastatic cell lines, while Smad4 expression was not seen in these cell lines.

Usefulness of the model as a tumor metastasis model for the evaluation of drugs. All of the highly metastatic cell lines served as highly reproducible models of peritoneal dissemination, and a quantitative relationship was observed between the number of inoculated cells and the animal survival rate (incidence of tumor) (data not shown). Next we evaluated antitumor effects of antitumor agents in this model. We selected CPT-11[17] and GEM[18] as representative cytotoxic agents. Figure 4A shows the survival curve of the 58As1 implanted mice treated with CPT-11. Most of the animals belonging to the untreated control group died of extensive peritoneal dissemination approximately 30 days after the implantation. In the CPT-11-treated group (200 mg/kg/head), however, 60 days passed before the first animal death was noted. Thus, treatment with CPT-11 significantly ($P < 0.001$, unpaired t-test) prolonged the survival of the animals injected with the tumor cells, and dose-dependency was evident when the data from multiple groups were compared. Similar results were also obtained for 44As3 cells (Fig. 4B). Figure 4(C) shows the results of the experiment in which GEM was administered intravenously following orthotopic inoculation of 58As1 cells. The survival period was significantly prolonged in the GEM-treated group (100 mg/kg/head). Similar results were also obtained for mice implanted with the 44As3 cells (data not shown).

To identify the stage of tumor metastasis suppressed by these agents, RT-PCR analysis was performed with sets of primers specific for human and mouse β actin, respectively. Cells collected from the intraperitoneal lavage fluid 21 days after orthotopic implantation of 58As1 cells served as the samples. Autopsy examination revealed that there was no macroscopic tumor formation in the gastric wall of the drug-treated animals, while peritoneal dissemination was noted in the untreated control group. Figure 4(D) shows two typical animals used for each experimental group. In the untreated control group, RT-PCR product represents human-derived β actin gene was clearly identified (lanes 3 and 4). In the CPT-11- and GEM-treated groups, however, the gene sequence of human origin was less clear (lanes 5, 6 and 7, 8, respectively). These results suggested that

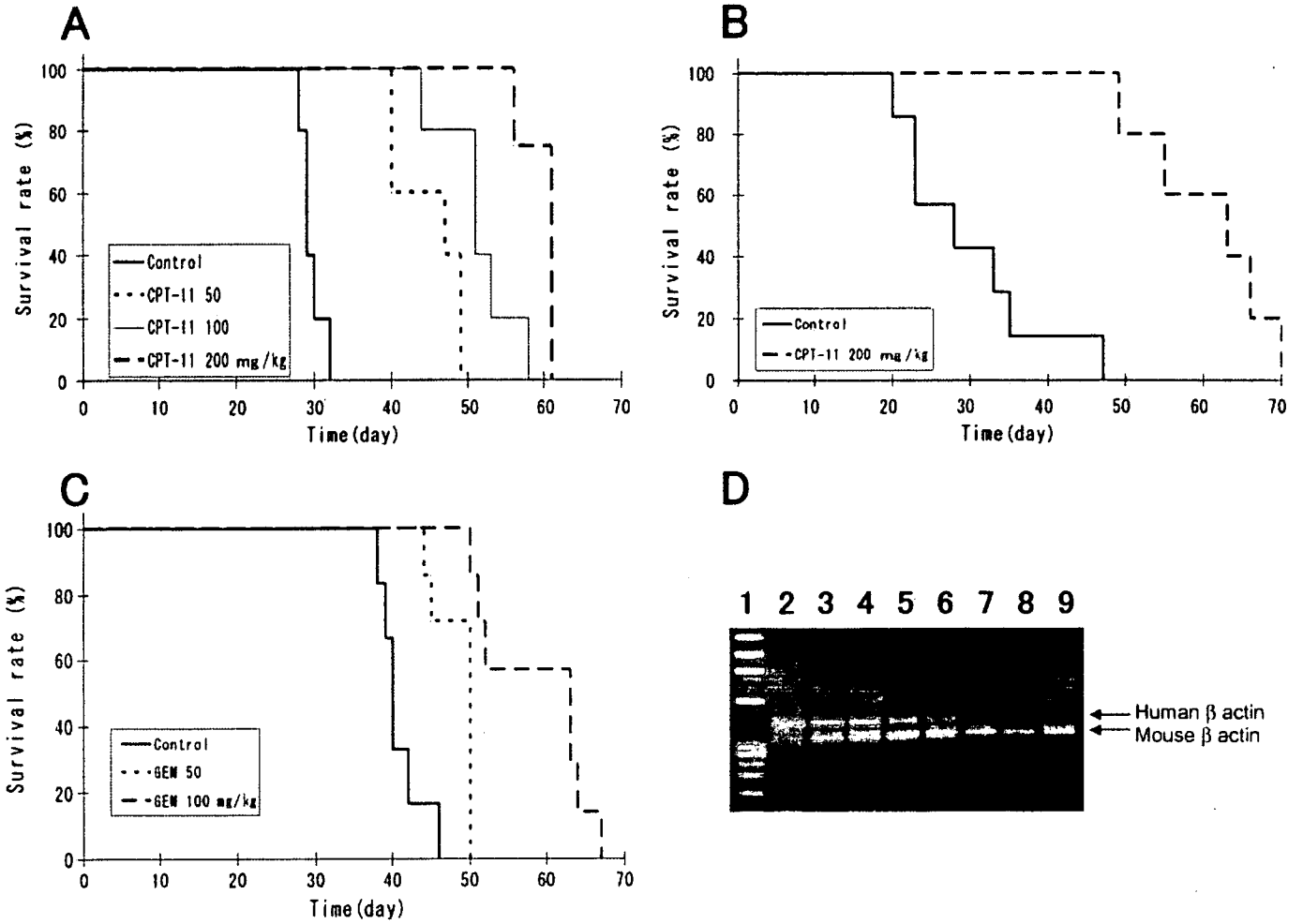

Fig. 4. Effects of CPT-11 and GEM in the peritoneal dissemination mouse model established using orthotopically implanted 44As3 or 58As1 cells. Mice receiving CPT-11 or GEM, or vehicle alone as control, were monitored daily for the development of peritoneal dissemination. (A), Survival of 58As1-tumor-bearing mice after CPT-11 treatment ($n = 5$; $P < 0.001$). This experiment was repeated thrice and similar results were observed each time. (B), Survival of 44As3-tumor-bearing mice after CPT-11 treatment ($n = 6$; $P < 0.001$). (C), Survival of 58As1-tumor-bearing mice after GEM treatment ($n = 7$; $P < 0.001$). Similar results were obtained in two independent experiments. (D), CPT-11 and GEM inhibit dissemination of cancer cells into the peritoneal cavity *in vivo*. RT-PCR was performed on the disseminated cells isolated from the intraperitoneal lavage fluid (2 mL of PBS) using human-specific and mouse-specific primers against β-actin. The total amount of RNA (200 ng) was equalized in all the samples. Lane 1, maker; lane 2, human gastric cell line HSC-39; lanes 3 and 4, untreated control group; lanes 5 and 6, 200 mg/kg CPT-11-treated group; lanes 7 and 8, 100 mg/kg GEM-treated group; lane 9, murine leukemia cell line P388.

treatment with the agents reduced the number of cancer cells in the peritoneal cavity. It was also found that the drugs directly inhibited the growth of s.c. tumors following implantation of 58As1 and 44As3 cells (data not shown). From these results, it is considered highly likely that while the agents suppress metastasis of these tumor cells by suppressing tumor formation at the implanted site, the small number of tumor cells remaining within the peritoneal cavity gradually proliferate, making it difficult to obtain better therapeutic results than some prolongation of the survival period.

Discussion

In the present study, we isolated 44As3 cells from HSC-44PE, and 58As1 and 58As9 cells from HSC-58, and succeeded, in a reliable manner, in establishing a model in which peritoneal dissemination occurred from a primary lesion of gastric carcinoma. The 44As3, 58As1 and 58As9 sublines were generated by the conventional method, that is by selection of highly metastatic clones (found in small numbers among cancer cells showing poor metastatic potential) *in vivo*.[19] On the basis of a study using clinical samples for microarray analysis of primary and metastatic lesions, investigators recently suggested that primary cancers with a high metastatic potential may differ in nature from those having a poor metastatic potential.[20] However, the results of our study support the conventional view that clones with a high metastatic potential contained in small amounts among the cancer tissues are responsible for the formation of metastatic lesions.

We consider that the establishment of this model is significant in the following respects: (i) it allows reproduction of all the steps in the development of cancerous peritonitis, from the stage of infiltrative growth of the tumor within the gastric mucosa to peritoneal dissemination and formation of ascites; (ii) it is an animal model of metastatic gastric cancer that closely resembles that in clinical cases; (iii) quantitative analysis is possible with this model, because it is established from cultured cells. The model is expected to be useful for the study of the continuity or association between infiltrative growth/peritoneal dissemination and gene expression, mechanism of formation of bloody ascites, and analysis of the microenvironmental factors influencing the development of the metastases. Comparison of the expression

 doi: 10.1111/j.1349-7006.2005.00054.x

levels of the relevant genes among different cell lines with markedly varying metastatic potential may be expected to allow isolation of new molecules involved in the peritoneal dissemination of tumors. Furthermore, these sublines are also expected to contribute to advancement of the functional analysis of the involvement of the newly identified molecules in peritoneal dissemination.

Following recent advances in the comprehensive analysis of gene expression, it has been gradually revealed that gene expression patterns undergo complex alterations during the course of metastasis of gastric carcinoma.[21–27] cDNA array analysis carried out using cell lines with varying metastatic potentials in the present study revealed altered expressions of numerous genes in these cells, including those involved in adhesion, proliferation and metabolism. Among others, markedly increased expression of the MMP1 gene[27,28] was observed in 44As3 cells; however, the expression of MMP1 at the protein level was low in these cells, suggesting that MMP1 may not be closely involved in metastasis. Cathepsin L, involved in the degradation of the extracellular matrix,[29] was intensely expressed in not only 44As3, but also 58As1 cells. This finding was confirmed by immunostaining. Intense cathepsin L expression was also seen in 58As9 cells. These results suggest that this molecule may be closely associated with the metastatic potential of these tumor cells. Meanwhile, it is known that invasion and metastasis of gastric cancer occur as a result of accumulation of changes in several genes.[21] These include genes encoding cell adhesion-related molecules (E-cadherin,[30,31] β-catenin,[30] integrin α6β4,[8] dysadherin,[32] CD44,[33,34] etc.), molecules associated with proliferation, loss of intercellular adhesion and matrix degradation (EGF, c-erbB-2,[35] cript,[36] etc.), motility-associated molecules (HGF, c-met,[37] etc.), molecules associated with vascularization (VEGF,[38] IL-6,[39] IL-8,[40] bFGF,[41] etc.), a tumor metastasis suppressor gene (nm23)[42] a gene associated with the malignant course of tumors (Smad),[43] and so on. When the expression of these genes was analyzed, markedly increased expression of MMP1, cathepsin L and nm23 was observed in the highly metastatic 44As3 cell line as compared with that in the poorly metastatic parent cell line. Molecules expressed specifically in the highly metastatic cell lines 58As1 and 58As9 included cathepsin L, dysadherin, CD44, integrin β4, EGFR, HGF and VEGF. Although these molecules seemed to be closely related to peritoneal dissemination of gastric carcinoma, it would be desirable to determine the exact causal relationship between these molecules and tumor metastasis using *in vivo* models. Nonetheless, our results suggest that: (i) there may be multiple pathways involving different molecules for the apparently single process of tumor metastasis, and (ii) the genes contributing to the metastatic potential of tumor cells may differ between the parent cells and the clones selectively isolated from it.

As stated, the presence of peritoneal metastasis represents an advanced stage of cancer associated with a poor prognosis, and no effective therapy for this condition is available as yet. It is therefore important to devise a new therapeutic strategy based on the aforementioned novel viewpoints. One such strategy that has been discussed is the development of anticancer agents based on molecular targeting. To seek such agents, a model allowing appropriate evaluation of drugs is essential, and models to be used for drug evaluation *in vivo* need to satisfy the following six requirements: (i) the tumor should undergo proliferation, spread, dissemination and metastasis akin to those seen in clinical cases; (ii) the tumor cell survival rate in the gastric wall following orthotopic implantation should be 100%; (iii) the frequency of metastasis should be 90–100%; (iv) the model should be highly reproducible; (v) the interindividual variance should be small, to allow easy comparison among different test groups; (vi) application to experiments using many animals should be relatively easy. When the animal model of peritoneal dissemination established in this study was evaluated according to these criteria, all the three highly metastatic cell lines established satisfied all of these six requirements. We evaluated the antitumor activities of two antitumor agents (CPT-11[17] and GEM[18]) using the animal models implanted with 58As1 and 44As3 cells. Treatment with these agents suppressed the proliferation and spread of the tumor and significantly prolonged the survival of the animals. For each of the cases studied, a dose-response relationship was observed, and the experiments were highly reproducible. Another advantage of this animal model is that the length of time from implantation to tumor formation is short (causing death within 40 days); this feature may be expected to contribute to shortening of the evaluation period. The advantages of this model may prove to be useful for the development of drugs based on molecular targeting.

In the past, no approach was known for isolation of host factors involved in the cascade of tumor proliferation in the primary lesion to formation of ascites, or for the functional analysis of this cascade (e.g. analysis of interactions). The model established in the present study is expected to contribute greatly to the advancement of studies in these fields and in other applied research.

Acknowledgments

We are grateful to Dr A. Ochiai (Pathology Division, National Cancer Center Research Institute East) for fruitful discussions. This study was supported in part by a Grant-in-Aid for Cancer Research from the Ministry of Health, Labor and Welfare of Japan.

References

1 Japanese Gastric Cancer Association. Japanese Classification of Gastric Carcinoma – 2nd English Edition. *Gastric Cancer* 1998; **1**: 10–24.
2 Tahara E. Endocrine tumors of the gastrointestinal tract: classification, function and biological behavior. In: Watanabe S, Wolff M, Sommers SC, eds. *Digestive Disease Pathology*. Philadelphia: Field andWood, 1988; 121–47.
3 Fenoglio-preier C, Carneiro F, Correa P *et al.* Gastric carcinoma. In: Hamilton SR, Aaltonen LA, eds. *World Health Organization Classification of Tumours. Pathology and Genetics of Tumours of the Digestive System*. Lyon: IARC Press, 2000; 37–52.
4 Maruyama K. Results of surgery correlated with staging. In: Preece PE, Cuschieri A, Wellwood JM, eds. *Cancer of the Stomach*. Orlando: Grune and Stratton, 1986; 145–63.
5 Moriguchi S, Maehara Y, Korenaga D, Sugimachi K, Nose Y. Risk factors which predict pattern of recurrence after curative surgery for patients with advanced gastric cancer. *Surg Oncol* 1992; **1**: 341–6.
6 Yashiro M, Chung YS, Nishimura S, Inoue T, Sowa M. Peritoneal metastatic model for human scirrhous gastric carcinoma in nude mice. *Clin Exp Metastasis* 1996; **14**: 43–54.
7 Fujita S, Suzuki H, Kinoshita M, Hirohashi S. Inhibition of cell attachment, invasion and metastasis of human carcinoma cells by anti-integrin β1 subunit antibody. *Jpn J Cancer Res* 1992; **83**: 1317–26.
8 Ishii Y, Ochiai A, Yamada T *et al.* Integrin α6β4 as a suppressor and a predictive marker for peritoneal dissemination in human gastric cancer. *Gastroenterology* 2000; **118**: 497–506.
9 Kotanagi H, Saito Y, Shinozawa N, Koyama K. Establishment of a human cancer cell line with high potential for peritoneal dissemination. *J Gastroenterol* 1995; **30**: 437–8.
10 Kaneko K, Yano M, Tsujinaka T *et al.* Establishment of a visible peritoneal micrometastatic model from a gastric adenocarcinoma cell line by green fluorescent protein. *Int J Oncol* 2000; **16**: 893–8.
11 Yanagihara K, Seyama T, Tsumuraya M, Kamada N, Yokoro K. Establishment and characterization of human signet ring cell gastric carcinoma cell lines with amplification of the c-myc oncogene. *Cancer Res* 1991; **51**: 381–6.
12 Yanagihara K, Kamada N, Tsumuraya M, Amano F. Establishment and characterization of a human gastric scirrhous carcinoma cell line in serum-free chemically defined medium. *Int J Cancer* 1993; **54**: 200–7.
13 Yanagihara K, Ito A, Toge T, Numoto M. Antiproliferative effects of

isoflavones on human cancer cell lines established from the gastrointestinal tract. *Cancer Res* 1993; **53**: 5815–21.
14 Yanagihara K, Tanaka H, Takigahira M *et al.* Establishment of two cell lines from human gastric scirrhous carcinoma that possess the potential to metastasize spontaneously in nude mice. *Cancer Sci* 2004; **95**: 575–82.
15 Luo L, Salunga RC, Guo H *et al.* Gene expression profiles of laser-captured adjacent neuronal subtypes. *Nat Med* 1999; **5**: 117–22.
16 Hughes TR, Mao M, Jones AR *et al.* Expression profiling using microarrays fabricated by an ink-jet oligonucleotide synthesizer. *Nat Biotechnol* 2001; **19**: 342–7.
17 Kanzawa F, Saijo N. *In vitro* interaction between gemcitabine and other anticancer drugs using a novel three-dimensional model. *Semin Oncol* 1997; **24**: S7-8–S7-16.
18 Saijo N. Preclinical and clinical trials of topoisomerase inhibitors. *Ann N Y Acad Sci* 2000; **922**: 92–9.
19 Fidler IJ. Rationale and methods for the use of nude mice to study the biology and therapy of human cancer metastasis. *Cancer Metast Rev* 1986; **5**: 29–49.
20 Ramaswamy S, Ross KN, Lander ES, Golub TR. A molecular signature of metastasis in primary solid tumors. *Nat Genet* 2003; **33**: 49–54.
21 Yokozaki H, Yasui W, Tahara E. Genetic and epigenetic changes in stomach cancer. *Int Rev Cytol* 2001; **204**: 49–95.
22 Yasui W, Oue N, Ito R, Kuraoka K, Nakayama H. Search for new biomarkers of gastric cancer through serial analysis of gene expression and its clinical implications. *Cancer Sci* 2004; **95**: 385–92.
23 Hippo Y, Yashiro M, Ishii M *et al.* Differential gene expression profiles of scirrhous gastric cancer cells with high metastatic potential to peritoneum or lymph nodes. *Cancer Res* 2001; **61**: 889–95.
24 Hippo Y, Taniguchi H, Tsutsumi S *et al.* Global gene expression analysis of gastric cancer by oligonucleotide microarrays. *Cancer Res* 2002; **62**: 233–40.
25 Hasegawa S, Furukawa Y, Li M *et al.* Genome-wide analysis of gene expression in intestinal-type gastric cancers using a complementary DNA microarray representing 23 040 genes. *Cancer Res* 2002; **62**: 7012–7.
26 Weiss MM, Kuipers EJ, Postma C *et al.* Genomic profiling of gastric cancer predicts lymph node status and survival. *Oncogene* 2003; **22**: 1872–9.
27 Inoue T, Yashiro M, Nishimura S *et al.* Matrix metalloproteinase-1 expression is a prognostic factor for patients with advanced gastric cancer. *Int J Mol Med* 1999; **4**: 73–7.
28 Sakurai Y, Otani Y, Kameyama K *et al.* Therole of stromal cells in the expression of interstitial collagenase (matrix metalloproteinase-1) in the invasion of gastric cancer. *J Surg Oncol* 1997; **66**: 168–72.
29 Dohchin A, Suzuki JI, Seki H, Masutani M, Shiroto H, Kawakami Y. Immunostained cathepsins B and L correlate with depth of invasion and different metastatic pathways in early stage gastric carcinoma. *Cancer* 2000; **89**: 482–7.
30 Hirohashi S. Inactivation of the E-cadherin-mediated cell adhesion system in human cancers. *Am J Pathol* 1998; **153**: 333–9.
31 Behrens J, Mareel MM, Van Roy FM, Birchmeier W. Dissecting tumor cell invasion: epithelial cells acquire invasive; properties after the loss of uvomorulin-mediated cell-cell adhesion. *J Cell Biol* 1989; **108**: 2435–47.
32 Ino Y, Gotoh M, Sakamoto M, Tsukagoshi K, Hirohashi S. Dysadherin, a cancer-associated cell membrane glycoprotein, down-regulated E-cadherin and promotes metastasis. *Proc Natl Acad Sci USA* 2002; **99**: 365–70.
33 Yokozaki H, Ito R, Nakayama H, Kuniyasu H, Taniyama K, Tahara E. Expression of CD44 abnormal transcripts in human gastric carcinomas. *Cancer Lett* 1994; **83**: 229–34.
34 Nishimura S, Chung YS, Yashiro M, Inoue T, Sowa M. CD44H plays an important role in peritoneal dissemination of scirrhous gastric cancer cells. *Jpn J Cancer Res* 1996; **87**: 1235–44.
35 Tsugawa K, Yonemura Y, Hirono Y *et al.* Amplification of the c-met, c-erbB-2 and epidermal growth factor receptor gene in human gastric cancers: correlation to clinical features. *Oncology* 1998; **55**: 475–81.
36 Kunuyasu H, Yoshida K, Yokozaki H *et al.* Expression of cript, a novel gene of the epidermal growth factor family, in human gastrointestinal carcinomas. *Jpn J Cancer Res* 1991; **82**: 969–73.
37 Kunuyasu H, Yasui W, Yokozaki H, Kitadai Y, Tahara E. Aberrant expression of c-met mRNA in human gastric carcinomas. *Int J Cancer* 1993; **55**: 72–5.
38 Takahashi Y, Cleary KR, Mai M, Kitadai Y, Bucana CD, Ellis LM. Significance of vessel count and vascular endothelial growth factor and its receptor (KDR) in intestinal-type gastric cancer. *Clin Cancer Res* 1986; **2**: 1679–84.
39 Huang SP, Wu MS, Wang HP, Yang PS, Kuo ML, Lin JT. Correlation between serum levels of interleukin-6 and vascular endothelial growth factor in gastric carcinoma. *J Gastroenterol Hepatol* 2002; **17**: 1165–9.
40 Kitadai Y, Haruma K, Sumii K *et al.* Regulation of angiogenesis in human gastric carcinomas by interleukin-8. *Am J Pathol* 1998; **152**: 93–100.
41 Ueki T, Koji T, Tamiya S, Nakane PK, Tsuneyoshi M. Expression of basic fibroblast growth factor and fibroblast growth factor in advanced gastric carcinoma. *J Pathol* 1995; **177**: 353–61.
42 Nakayama H, Yasui W, Yokozaki H, Tahara E. Reduced expression of nm23 is associated with metastasis of human gastric carcinomas. *Jpn J Cancer Res* 1993; **84**: 184–90.
43 Ijichi H, Ikenoue T, Kato N *et al.* Systemic analysis of the TGF-beta-smad signaling pathway in gastrointestinal cancer cells. *Biochem Biophys Res Commun* 2001; **289**: 350–7.

 doi: 10.1111/j.1349-7006.2005.00054.x

Enhancement of Sensitivity to Tumor Necrosis Factor α in Non–Small Cell Lung Cancer Cells with Acquired Resistance to Gefitinib

Koichi Ando,[1] Tohru Ohmori,[1,2] Fumiko Inoue,[2] Tsuyoki Kadofuku,[2] Takamichi Hosaka,[1] Hiroo Ishida,[1] Takao Shirai,[1] Kentaro Okuda,[1] Takashi Hirose,[1] Naoya Horichi,[1] Kazuto Nishio,[3] Nagahiro Saijo,[3] Mitsuru Adachi,[3] and Toshio Kuroki[4]

Abstract Tumor cells that have acquired resistance to gefitinib through continuous drug administration may complicate future treatment. To investigate the mechanisms of acquired resistance, we established PC-9/ZD2001, a non-small-cell lung cancer cell line resistant to gefitinib, by continuous exposure of the parental cell line PC-9 to gefitinib. After 6 months of culture in gefitinib-free conditions, PC-9/ZD2001 cells reacquired sensitivity to gefitinib and were established as a revertant cell line, PC-9/ZD2001R. PC-9/ZD2001 cells showed collateral sensitivity to several anticancer drugs (vinorelbine, paclitaxel, camptothecin, and 5-fluorouracil) and to tumor necrosis factor α (TNF-α). Compared with PC-9 cells, PC-9/ZD2001 cells were 67-fold more sensitive to TNF-α and PC-9/ZD2001R cells were 1.3-fold more sensitive. Therefore, collateral sensitivity to TNF-α was correlated with gefitinib resistance. PC-9/ZD2001 cells expressed a lower level of epidermal growth factor receptor (EGFR) than did PC-9 cells; this down-regulation was partially reversed in PC-9/ZD2001R cells. TNF-α-induced autophosphorylation of EGFR (cross-talk signaling) was detected in all three cell lines. However, TNF-α-induced Akt phosphorylation and IκB degradation were observed much less often in PC-9/ZD2001 cells than in PC-9 cells or PC-9/ZD2001R cells. Expression of the inhibitor of apoptosis proteins c-IAP1 and c-IAP2 was induced by TNF-α in PC-9 and PC-9/ZD2001R cells but not in PC-9/ZD2001 cells. This weak effect of EGFR on Akt pathway might contribute to the TNF-α sensitivity of PC-9/ZD2001 cells. These results suggest that therapy with TNF-α would be effective in some cases of non-small-cell lung cancer that have acquired resistance to gefitinib.

Gefitinib (Iressa, ZD1839), a small-molecule epidermal growth factor receptor (EGFR) tyrosine kinase inhibitor, has been approved for the treatment of refractory and relapsed non-small-cell lung cancer (NSCLC) patients in a number of countries around the world. This drug, which is given continuously as a once-daily oral dose, showed antitumor activity in patients with relapsed or recurrent NSCLC; however, tumor responses were observed in 12% to 18% of patients with chemotherapy-refractory advanced NSCLC (1, 2). Even in cases sensitive to gefitinib, resistance might be acquired through continuous drug administration. Additional treatments for cases of NSCLC relapsing during treatment with gefitinib are urgently needed.

To investigate the mechanism of acquired resistance to gefitinib, we previously established gefitinib-acquired resistant cells, PC-9/ZD2001, from a NSCLC, PC-9, which is hypersensitive to gefitinib and has a 15-del mutation in exon 19 of EGFR (data not shown). After >6 months of culture in gefitinib-free conditions, the sensitivity of PC-9/ZD2001 cells to gefitinib was restored, and the cells were subsequently established as a revertant cell line, PC-9/ZD2001R. The active mutation of EGFR was sustained in both the resistant and the revertant cell lines and the existence of revertant cell line suggests the additional mutation of EGFR, such as a secondary mutation of T790M in EGFR that causes resistance to gefitinib (3, 4), is unlikely to be contribute to this gefitinib resistance. In the gefitinib-resistant cells, the expression levels of EGFR and mRNA decreased to 30% to 50% of those in parental cells. A ligand-induced EGFR activation minimally activated mitogen-activated protein kinase signaling pathways and the inhibitory effect of gefitinib on this

Authors' Affiliations: [1]First Department of Internal Medicine and [2]Institute of Molecular Oncology, Showa University, Tokyo, Japan; [3]Internal Medicine, Pharmacology Division, National Cancer Center Hospital, National Cancer Center Research Institute, Tokyo, Japan; and [4]Gifu University, Gifu, Japan

Received 4/12/05; revised 8/10/05; accepted 8/26/05.

Grant support: Grant-in-Aid for a High-Technology Research Center Project from the Ministry of Education, Science, Sports, and Culture of Japan; Showa University Grant-in-Aid for Innovative Collaborative Research Projects; and Special Research Grant-in-Aid for Development of Characteristic Education from the Ministry of Education, Culture, Sports, Science, and Technology of Japan.

The costs of publication of this article were defrayed in part by the payment of page charges. This article must therefore be hereby marked *advertisement* in accordance with 18 U.S.C. Section 1734 solely to indicate this fact.

Requests for reprints: Tohru Ohmori, Institute of Molecular Oncology, Showa University, Hatanodai, 1-5-8, Shinagawa-ku, Tokyo 142-8555, Japan. Fax: 81-3-3784-2299; E-mail: ohmorit@med.showa-u.ac.jp.

doi:10.1158/1078-0432.CCR-05-0811

pathway was significantly decreased in the resistant cells.[5] To elucidate the cross-resistance to other anticancer agents, we examined the sensitivity to the conventional anticancer agents and tumor necrosis factor α (TNF-α). PC-9/ZD2001 showed cross-resistance to another EGFR inhibitor, AG1478. Interestingly, gefitinib-resistant cells were ~3-fold more sensitive than PC-9 cells to the cytotoxic effects of vinorelbine, paclitaxel, camptothecin, 5-fluorouracil, and a cytokine, TNF-α.[5] The same tendency was confirmed in the other gefitinib-resistant clones established along with PC-9/ZD2001. The restoration of these collateral sensitivities (except 5-fluorouracil) in revertant PC-9/ZD2001R cells suggests that such sensitivities are correlated with the mechanism of gefitinib resistance.

TNF-α is the prototype of ~20 related cytokines that act through specific members of the TNF receptor (TNFR) super family (5–7). Several cancer therapies exploiting the cytotoxic effect of TNF-α on solid tumors and soft-tissue sarcomas have recently been examined in clinical trials (8, 9). The TNF-α stimulates inflammation by turning on gene transcription through signaling cascades such as the Akt/nuclear factor κB (NF-κB) pathway. This signaling subsequently serves as the primary mechanism to protect cells against apoptotic stimuli through several transcriptional genes, such as inhibitor of apoptosis proteins (IAP), the specific inhibitor of caspases (10, 11). In contrast, TNF-α-mediated signaling also triggers apoptosis through the activation of caspase-8 and the downstream caspase-3 or caspase-7 in a wide variety of cells (12). From these observations, it is possible to say that TNF-α has two different signaling pathways that contradict each other. The cytotoxic effect of TNF-α might be determined by ratios between the apoptosis-inducing and the apoptosis-inhibiting effects.

Akt/NF-κB signaling also occurs downstream of EGFR and this signaling mediates cell proliferation and antiapoptotic signaling through this pathway (13). In the case of the antiapoptotic signaling of TNF-α, TNFR is known to activate Akt/NF-κB in three ways: directly through phosphatidylinositol 3-kinase activation, or indirectly through cross-talk signaling to EGFR, or both together (5–7, 12, 14, 15). Moreover, several recent articles report that the TNFR-mediated cross-talk signaling to EGFR occurs in a ligand-dependent and -independent manner (16–21). Therefore, to investigate the mechanisms of the collateral sensitivity to TNF-α in gefitinib-acquired resistant cells, we focused on TNF-α-induced cross-talk signaling to EGFR and analyzed the Akt/NF-κB signaling pathway in response to TNF-α.

In this article, we show that a weakness of Akt/NF-κB signaling from TNF-α-mediated cross-talk signaling via EGFR causes the collateral sensitivity to TNF-α in the gefitinib-acquired resistant cell line. Moreover, this cross-talk signaling is thought to be a dominant pathway of TNF-α-mediated Akt activation.

Materials and Methods

Chemicals and antibodies. Gefitinib was donated by AstraZeneca Pharmaceuticals (Wilmington, DE). An anti-phospho-EGFR antibody (Tyr1068) was purchased from Cell Signaling Technology (Beverly, MA). Other antibodies and chemicals were purchased from Santa Cruz Biotechnology, Inc. (Santa Cruz, CA) and Sigma-Aldrich Co. (St. Louis, MO), respectively, unless otherwise specified.

Cell lines and cultures. The PC-9 human NSCLC cell line, established from a previously untreated patient, was kindly donated by Prof. K. Hayata (Tokyo Medical College, Tokyo, Japan.). The PC-9 cells were cultured with RPMI 1640 supplemented with 10% FCS and maintained in a 5% CO_2 incubator at 37°C under humidified conditions.

Establishment of gefitinib-resistant cell lines. To establish gefitinib-resistant cell lines, PC-9 cells were continuously exposed to increasing dosages of gefitinib for >1 year. The surviving cells were cloned and three gefitinib-resistant cell lines, designated as PC-9/ZD2001, PC-9/ZD2002, and PC-9/ZD2003, were established. These cell lines can survive exposure to 200 nmol/L gefitinib. Sensitivity to gefitinib was restored by culture of PC-9/ZD2001 in gefitinib-free conditions for >6 months. The restored cells were cloned and subsequently established as a revertant cell line, PC-9/ZD2001R.

Established resistant cell lines were maintained by culture in a medium containing 200 nmol/L gefitinib. To eliminate the effects of gefitinib, the resistant cells were cultured in a drug-free medium for at least 2 weeks before all experiments. As the relative resistance values of these cell lines were stable for at least 3 months after culture under drug-free conditions (data not shown), we used the cells for experiments during this period.

Growth inhibition assay. To measure sensitivity to gefitinib, a 3-(4,5-dimethylthiazol-2-yl)-2,5-diphenyltetrazolium bromide assay was done (Cell Titer 96 assay kit, Promega Corp., Madison, WI). In brief, PC-9, PC-9/ZD2001, and PC-9/ZD2001R cells were seeded onto 96-well plates and preincubated overnight. The cells were continuously exposed to the indicated concentrations of gefitinib for 4 or 5 days. Absorbance was measured at 570 nm with a microplate reader (Model 550, Bio-Rad Laboratories, Hercules, CA).

Analysis of tumor necrosis factor α–induced apoptotic cell death. The PC-9, PC-9/ZD2001, and PC-9/ZD2001R cells were treated with 100 ng/mL TNF-α for the indicated time periods. They were then fixed with 4% paraformaldehyde at 4°C for 30 minutes. After 100 μL of 70% ethanol were added, the cells were permeabilized by incubation overnight at −20°C. Apoptotic DNA fragments were probed with the terminal deoxyribonucleotidyl transferase-mediated dUTP nick end labeling method (MEBSTAIN Apoptosis TUNEL Kit Direct, Medical & Biological Laboratories, Nagoya, Japan) and subpopulations of apoptotic cells were measured with a flow cytometer (FACSCalibur, BD Biosciences Immunocytometry Systems, San Jose, CA).

Activity assays for CPP32/caspase-3 and FLICE/caspase-8. Activities of CPP32/caspase-3 and FLICE/caspase-8 were measured with caspase-3 and caspase-8 colorimetric assay kits (MRL Diagnostics, Cypress, CA) according to the instructions of the manufacturer. The PC-9, PC-9/ZD2001, and PC-9/ZD2001R cells were incubated for 12 hours with 10 ng/mL TNF-α and then resuspended in 50 μL of chilled cell lyses buffer. The cells were incubated on ice for 10 minutes and the protein concentration of the supernatant was assayed with a bicinchoninic acid protein assay kit (Sigma-Aldrich). A certain amount of each sample was added to 50 μL of 2× reaction buffer containing the respective substrates DEVD-pNA and IETD-pNA, then incubated at 37°C for 1 hour. After incubation, absorbance was measured at 400 and 405 nm with a microtiter plate reader (Model 550, Bio-Rad Laboratories).

Immunoblot analysis. Cells were treated with 10 ng/mL of TNF-α for 30 minutes, then washed twice with ice-cold PBS and lysed in EBC buffer [50 mmol/L Tris-HCl (pH 8.0), 120 mmol/L NaCl, 0.5% NP40, 100 μmol/L NaF, 200 μmol/L Na orthovanadate, and 10 μg/mL of leupeptin, aprotinin, and phenylmethylsulfonyl fluoride] with an ultrasonic disrupter (Tomy Digital Biology Co., Ltd., Tokyo, Japan). The cell lysate was precleared by centrifugation, resolved by 10% SDS-PAGE, transferred to nitrocellulose membrane, and probed with antibodies against EGFR, phospho-EGFR (Tyr1045), phosphatase and tensin homologue, Akt, phospho-Akt, IκB, c-IAP1, and c-IAP2. Bound antibodies were detected with horseradish peroxidase-linked immunoglobulin (Amersham Biosciences, Buckinghamshire, United Kingdom)

[5] T. Yamaoka, T. Ohmori, F. Inoue, et al. Characteristics of gefitinib-acquired resistance in non–small cell lung cancer cell lines, submitted for publication.

and enhanced chemiluminescence reagents (Perkin-Elmer Life and Analytical Sciences, Boston, MA).

Real-time reverse transcription-PCR method. Total RNA was isolated with the guanidium isothiocyanate method using an RNA purification kit (RNeasy Mini Kit, Qiagen, Venlo, the Netherlands) according to the instructions of the manufacturer. After RNA isolation, cDNA was prepared in the presence of random 9-mers with a reverse transcription-PCR (RT-PCR) kit (Takara Shuzo Co., Ltd., Kyoto, Japan). Expression levels of EGFR, c-IAP1, and c-IAP2 mRNA were quantified with a fluorescence-based real-time detection method (GeneAmp 5700 Sequence Detection System, Applied Biosystems, Foster City, CA). Cycling conditions were 40 cycles at 94°C for 20 seconds, 55°C (EGFR) and 64°C (c-IAPs) for 20 seconds, and 72°C for 30 seconds. Expression of the mRNA was measured with the following primer sets: EGFR, 5′-ACGAATGGGCCTAAGATC-3′ and 5′-TGCTTACCCGGATTCTAGG-3′; c-IAP1, 5′-ATGTGGGTAACAGTGATGATGTCA-3′ and 5-AAACCAC-TTGGCATGTTGAAC-3′; and c-IAP2, 5′-CTAGTGTTCATGTTGAAC-3′ and 5′-CCTCAAGCCACCATCACAAC-3′. The expression of β-actin mRNA was used as an internal control.

Statistical analysis. Statistical analysis was done with the StatView II software program (Abacus Concepts, Berkeley, CA). Activities of CPP32/caspase-3 and FLICE/caspase-8 were analyzed with paired Student's t test. $P < 0.05$ was considered significant.

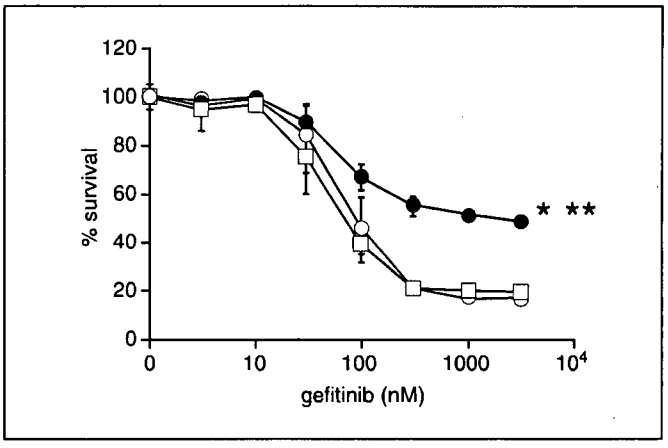

Fig. 1. Cytotoxic effects of gefitinib in a gefitinib-resistant NSCLC cell line. The cells (2×10^3 per well) were seeded onto a 96-well plate and preincubated overnight, then continuously exposed to the indicated concentrations of gefitinib for 4 or 5 days. The growth inhibition rate was analyzed with 3-(4,5-dimethylthiazol-2-yl)-2,5-diphenyltetrazolium bromide assay as described in Materials and Methods. ○, PC-9; ●, PC-9/ZD2001; □, PC-9/ZD2001R. Points, mean of three different experiments; bars, SD. *, $P < 0.001$, PC-9 versus PC-9/ZD2001; **, $P < 0.001$, PC-9/ZD2001R versus PC-9/ZD2001.

Results

Establishment of acquired gefitinib-resistant cell lines. To elucidate the mechanism of acquired resistance against gefitinib, we established gefitinib-resistant NSCLC cell lines through continuous exposure of this drug. Resistance against gefitinib developed quite slowly; the relative resistant values of 3- to 4-fold were reached after >1-year exposure to gefitinib. We picked the clones of gefitinib-resistant cell lines named PC-9/ZD2001, PC-9/ZD2002, and PC-9/ZD2003. These cell lines can survive in 200 nmol/L gefitinib-contained medium. Sensitivities to gefitinib were measured by 3-(4,5-dimethylthiazol-2-yl)-2,5-diphenyltetrazolium bromide assay. In the case of PC-9/ZD2001 cells, the cell line was able to survive by >50% at the concentration of >500 nmol/L gefitinib. This concentration caused maximum inhibition in PC-9. The IC_{40} value of gefitinib in PC-9 cells was 53.0 ± 8.1 nmol/L. The gefitinib-resistant cell line PC-9/ZD2001 showed a 4-fold higher resistance to gefitinib than PC-9 cells (IC_{40} = 211.1 ± 32.4 nmol/L; Fig. 1). Culture of the cells in gefitinib-free conditions for 6 months restored sensitivity to gefitinib in PC-9/ZD2001 and subsequently established a revertant cell line, PC-9/ZD2001R, in which sensitivity to gefitinib was completely restored (IC_{40} = 46.3 ± 10.2 nmol/L).

Analysis for tumor necrosis factor α-induced apoptotic cell death. TNF-α-induced cytotoxic effect was measured by 3-(4,5-dimethylthiazol-2-yl)-2,5-diphenyltetrazolium bromide assay. The IC_{40} values of TNF-α in PC-9, PC-9/ZD2001, and PC-9/ZD2001R cell lines were 815.0 ± 44.8, 12.2 ± 1.4, and 626.2 ± 18.5 ng/mL, respectively. PC-9/ZD2001 cells acquired new sensitivity to TNF-α. PC-9/ZD2001 was ~67-fold more sensitive to TNF-α as compared with PC-9, but this sensitization was restored to 1.3-fold in PC-9/ZD2001R (Fig. 2A). This collateral sensitivity to TNF-α was confirmed in the other gefitinib-resistant cell lines, PC-9/ZD2002 and PC-9/ZD2003 (data not shown).

Additionally, we measured TNF-α-induced apoptotic cell death by flow cytometry. The apoptotic cells were stained by the terminal deoxyribonucleotidyl transferase-mediated dUTP nick end labeling method. No significant apoptosis was observed in these three cell lines until 24 hours of exposure to TNF-α (10 ng/mL). Forty-eight hours of TNF-α exposure induced a 6-fold higher apoptotic cell death in PC-9/ZD2001 cells (70.3%) as compared with the parental PC-9 cells (11.8%). This enhancement was completely recovered in PC-9/ZD2001R cells (16.6%; Fig. 2B; Table 1). These results suggest that the collateral sensitivity to TNF-α might be correlated with the resistance to gefitinib in these cell lines.

Analysis of tumor necrosis factor α-mediated activations of CPP/caspase-3 and FLICE/caspase-8. To clarify the difference of TNF-α-induced apoptotic cell death in these cell lines, we analyzed TNF-α-mediated CPP32/caspase-3 and its upstream FLICE/caspase-8 activations by caspase-8 and caspase-3 colorimetric protease assay kits (Medical and Biological Laboratories), respectively. PC-9, PC-9/ZD2001, and its revertant PC-9/ZD2001R cells were incubated with the indicated concentrations of TNF-α for 12 hours. In the case of caspase-3, TNF-α did not cause any increases in the activity in PC-9 and PC-9/ZD2001R cells even at the highest concentration of 100 ng/mL. In contrast, TNF-α significantly enhanced caspase-3 activity in PC-9/ZD2001 cells even at the concentration of 1 ng/mL within this time course (Fig. 3A). In the case of caspase-8, TNF-α enhanced the activities in all three cell lines from 10 ng/mL (Fig. 3B). TNF-α at 100 ng/mL activated caspase-8 ~1.6-, 2.9-, and 1.9-fold higher in PC-9, PC-9/ZD2001, and PC-9/ZD2001R, as compared with the respective untreated cells. In PC-9/ZD2001 cells, TNF-α caused the highest relative induction of caspase-8 (Fig. 3B).

Immunoblot analysis for the tumor necrosis factor α-induced cross-talk signaling to epidermal growth factor receptor and Akt/nuclear factor κB pathway activation. EGFR expression was significantly lower in PC-9/ZD2001 than in PC-9 cells (Fig. 4A). When measuring the expression of EGFR protein by a densitometer (calculated by the NIH image software), the expression was decreased to 52.4 ± 2.6% of that in parental cell line. Moreover, we measured the expression levels of EGFR mRNA by a real-time RT-PCR method. The expression level in PC-9/ZD2001 was decreased to 37.0 ± 3.2% of that in parental

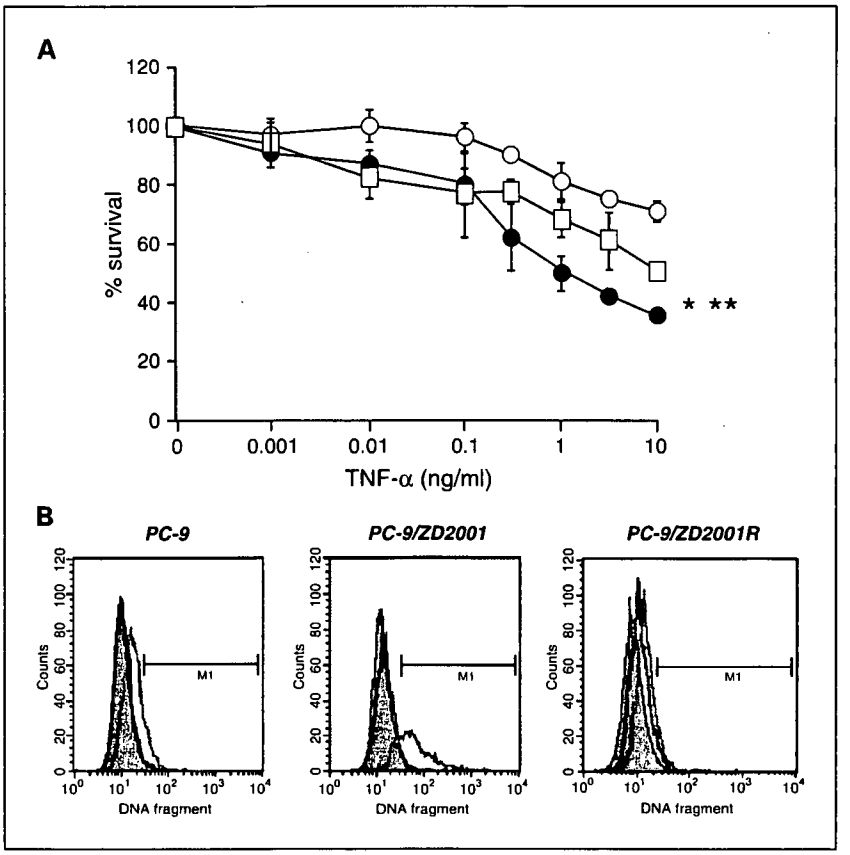

Fig. 2. Gefitinib-resistant cells acquired sensitivity to TNF-α. *A*, the cells were continuously treated with the indicated concentrations of TNF-α for 4 or 5 days. The growth inhibition rate was analyzed with 3-(4,5-dimethylthiazol-2-yl)-2,5-diphenyltetrazolium bromide assay as described in Materials and Methods. ○, PC-9; ●, PC-9/ZD2001; □, PC-9/ZD2001R. PC-9/ZD2001 cells were ~67-fold more sensitive to TNF-α than were PC-9 cells but the sensitivity of revertant PC-9/ZD2001R cells decreased to 1.3-fold that in PC-9 cells. Points, mean of three different experiments; bars, SD. *, $P < 0.001$, PC-9 versus PC-9/ZD2001; **, $P < 0.001$, PC-9/ZD2001R versus PC-9/ZD2001. *B*, the cells were treated with 10 ng/mL TNF-α for the indicated time periods. After treatment, the cells were fixed with 4% paraformaldehyde at 4°C and permeabilized with 70% ethanol. Fragments of apoptotic DNA were stained with the terminal deoxyribonucleotidyl transferase-mediated dUTP nick end labeling method and measured with flow cytometry as described in Materials and Methods.

cells. The same down-regulation of EGFR was seen in the other resistant cell lines (data not shown). In the case of PC-9/ZD2001R, expression levels of EGFR protein and mRNA were also decreased to 69.3 ± 1.1% and 56.8 ± 2.2%, respectively, as compared with PC-9. The expression of EGFR was restored, but not completely, in the revertant cell line.

In PC-9 cells, cross-talk signaling from TNFR to EGFR was observed and treatment with 10 ng/mL TNF-α for 30 minutes induced significant autophosphorylation of EGFR (Fig. 4A). According to the autophosphorylation of EGFR, definite phosphorylation of Akt and a decrease in IκB content were observed. The activation of Akt and down-regulation of IκB were inhibited by gefitinib at concentrations <10 nmol/L. Because gefitinib (100 nmol/L) mostly inhibited this signaling, we concluded that the cross-talk signaling from TNFR to EGFR might be the dominant pathway of TNF-α-mediated Akt/NF-κB activation in this cell line rather than the direct signaling from TNFR to Akt. In contrast, although EGFR autophosphorylation was observed, only partial phosphorylation of Akt and down-regulation of IκB, compared with those in PC-9, were observed after TNF-α exposure in PC-9/ZD2001 cells (Fig. 4A and B). Treatment with gefitinib inhibited this cross-talk signaling to EGFR but had no effect on downstream Akt phosphorylation.

These observations suggest that TNF-α-mediated EGFR signaling has less effect on the Akt/NF-κB pathway in the gefitinib-resistant PC-9/ZD2001 cell line. Other stimuli might activate Akt in an EGFR-independent manner. In the revertant PC-9/ZD2001R cell line, this weak effect of EGFR was largely reversed and TNF-α exposure induced autophosphorylation of EGFR and subsequent activation of the Akt/NF-κB pathway. The expression levels of phosphatase and tensin homologue, a suppressor of Akt signaling, did not differ significantly among PC-9, PC-9/ZD2001, and PC-9/ZD2001R cells. This decreased effect of EGFR might be partially caused by the down-regulation of EGFR expression in PC-9/ZD2001. However, although the EGFR-mediated signaling and the resistance to gefitinib were mostly restored, EGFR expression remained only partially restored in PC-9/ZD2001R. For this reason, we speculated that the down-regulation of EGFR expression might not fully explain the weak EGFR signaling to Akt pathway in PC-9/ZD2001 cells.

To clarify the decreased EGFR signaling in PC-9/ZD2001, we examined the inhibitory effect of a phosphatidylinositol 3-kinase inhibitor, wortmannin, on the TNF-α-induced activation of this pathway (Fig. 4B). Interestingly, wortmannin inhibited the TNF-α-mediated phosphorylation of Akt in PC-9/ZD2001 cells at the same level as it did in PC-9 and PC-9/ZD2001R cells.

Expresstion of c-IAP1 and c-IAP2 on treatment with tumor necrosis factor α. After treatment with TNF-α (10 ng/mL) for 30 minutes, expression of c-IAP1 and c-IAP2 proteins was

Table 1. Percentage of apoptotic subpopulations

%Apoptosis	PC-9	PC-9/2001	PC-9/2001R
Control	1.1	1.2	1.1
24 h	1.4	2.3	3.2
48 h	11.8	70.3	6.6

NOTE: After 72 hours of exposure to TNF-α, significant apoptotic cell death was observed in PC-9/ZD2001 cells but not in PC-9 or PC-9/ZD2001R cells.

significantly increased in PC-9 and PC-9/ZD2001R cells but not in PC-9/ZD2001 cells (Fig. 4A and B). According to the results of Akt phosphorylation, induction was inhibited by gefitinib in PC-9 and PC-9/ZD2001R cells but not in PC-9/ZD2001 cells. Wortmannin could inhibit induction in all three cell lines. Consistent with the results of protein expression, treatment with TNF-α increased the expression level of c-IAP1 and c-IAP2 mRNA in PC-9 and PC-9/ZD2001R cells in a dose-dependent manner (Fig. 5A and B). After treatment with 100 ng/mL TNF-α for 12 hours, the expression levels of both c-IAP1 and c-IAP2 mRNA were significantly increased in PC-9 cells (c-IAP1, 7.05 ± 0.62; c-IAP2, 18.22 ± 0.25) and PC-9/ZD2001R cells (c-IAP1, 7.02 ± 0.54; c-IAP2, 11.56 ± 0.75) but not in PC-9/ZD2001 cells (c-IAP1, 2.60 ± 0.58; c-IAP2, 2.83 ± 0.66). These observations suggest that TNF-α-induced apoptotic signaling is not inhibited by its own antiapoptotic effects, such as IAPs induction, owing to the weak effect of TNF-α-mediated signaling and the Akt/NF-κB pathway via EGFR in this gefitinib-resistant cell line.

Discussion

We have shown that the gefitinib-acquired resistant NSCLC cell line PC-9/ZD2001 acquired collateral sensitivity to the apoptotic effect of TNF-α. Because this collateral sensitivity was significantly diminished in the revertant PC-9/ZD2001R, it might be correlated with gefitinib resistance. As described before, PC-9/ZD2001 also acquired collateral sensitivities to some anticancer drugs, such as vinorelbine, paclitaxel, camptothecin, and 5-fluorouracil. However, this cell line did not show the collateral sensitivities to cisplatin, etoposide, mitomycin C, and cyclophosphamide.[5] Moreover, there was no difference of susceptibility to serum-starved condition between PC-9 and PC-9/ZD2001 (data not shown). From these observations, it can be concluded that the collateral sensitivities of the gefitinib-resistant cells are specific to some cell stresses and are not caused by the fragility of the cells. Because the same tendency of sensitivity was seen in the other resistant clones, PC-9/ZD2002 and PC-9/ZD2003, the acquired sensitivity to the anticancer drugs and TNF-α could be a general phenomenon even in the clinical gefitinib-resistant cells.

TNF-α activates not only apoptotic signaling but also antiapoptotic signaling via the Akt/NF-κB activation (22, 23). Activation of the downstream transcription factor NF-κB inhibits various types of apoptotic cell death by inducing apoptotic inhibitory proteins (22, 23), such as bcl-2 (24), bcl-xl (25), forkhead (26), and IAPs (10, 11, 27, 28). As described before, it is thought that the cytotoxic effect of TNF-α is determined by ratios between the apoptosis-inducing and the apoptosis-inhibiting effects (5–7, 12, 14, 15).

In parental PC-9 cells, TNF-α induced EGFR autophosphorylation and subsequent Akt/NF-κB pathway activation (Fig. 4A and B). This autophosphorylation was completely inhibited by a low concentration of gefitinib (10 nmol/L). From these observations, we think that TNF-α-induced Akt/NF-κB pathway activation occurs mainly through cross-talk from TNFR to EGFR in this cell line. Because the expression level of EGFR was significantly decreased in PC-9/ZD2001 as compared with the parental PC-9, the decline of the cross-talk signaling might partially diminish the TNF-α-induced activation of the Akt/NF-κB pathway. Our results are supported by those of an earlier study showing that resistance to the cytotoxic effect of TNF-α is associated with high expression of Her family receptors, such as EGFR (Her1), erbB2/Her2/neu, or Her3, in a panel of human tumor cell lines (29). However, the decreased EGFR signaling from the Akt/NF-κB pathway could not be fully explained by the lower EGFR expression in PC-9/ZD2001 because EGFR expression remained only partially restored in the revertant PC-9/ZD2001R cell line. In light of these observations, to clarify the mechanisms of collateral sensitivity to TNF-α in the gefitinib-resistant cells, we focused on the cross-talk signaling from TNFR to EGFR in PC-9, PC-9/ZD2001, and PC-9/ZD2001R cells.

Several recent articles have reported that TNFR mediates cross-talk signaling to EGFR through a ligand-dependent and -independent manner (16–19, 21, 23). Chan et al. (17) have reported that exposure of human mammary epithelial cells to TNF-α results in transactivation of EGFR through metalloprotease-dependent shedding of EGFR ligand(s). Hirota et al. (18) reported that EGFR transactivation by TNF-α is

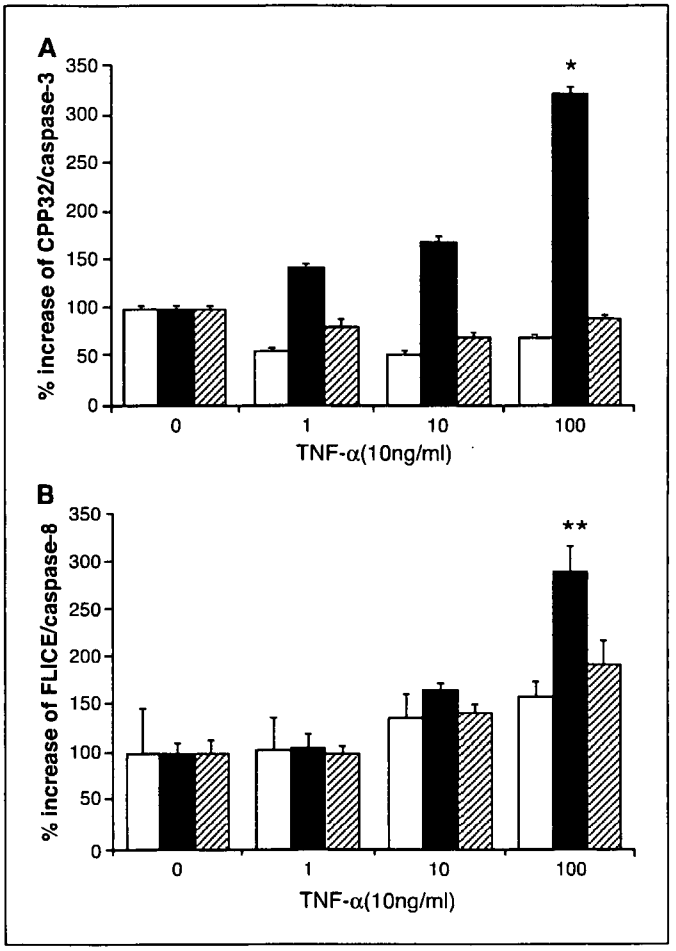

Fig. 3. TNF-α-mediated activation of CPP32/caspase-3 and FLICE/caspase-8 in PC-9, PC-9/ZD2001, and PC-9/ZD2001R cells. Activation of CPP32/caspase-3 and FLICE/caspase-8 was measured as described in Materials and Methods. The cells were exposed to the indicated concentrations of TNF-α for 12 hours; after which equivalent amounts of samples were reacted with the substrates DEVD-pNA and IETD-pNA. Absorbance was measured at 400 and 405 nm with a microtiter plate reader. *A*, CPP32/caspase-3. *B*, FLICE/caspase-8. TNF-α activated FLICE/caspase-8 in all three cell lines but activated CPP32/caspase-3 only in PC-9/ZD2001 cells. Data calculated as the percentage increase compared with respective untreated controls. Points, mean of three different experiments each done in triplicate; bars, SD. Open columns, PC-9; closed columns, PC-9/ZD2001; hatched columns, PC-9/ZD2001R. *, $P < 0.001$, PC-9 versus PC-9/ZD2001. **, $P = 0.02$, PC-9 versus PC-9/ZD2001.

regulated by means of redox-dependent mechanisms. The transactivation of EGFR was observed to occur quickly, after <30 minutes of exposure to TNF-α in PC-9 cells (Fig. 4A and B). No additional induction of ligands, EGF and transforming growth factor-α, were detected by ELISA in the culturing medium of the cells even after 6 hours of 100 ng/mL TNF-α exposure (data not shown). From these observations, we think that this activation could occur independently of ligands but not through TNF-α-mediated ligands synthesis or proteolytic releasing of preexisting ligands from the disrupted cells. Although TNF-α induced the same levels of EGFR autophosphorylation in all three cell lines, this EGFR activation is minimally transmitted to the downstream Akt/NF-κB pathway in the resistant PC-9/ZD2001 cells (Fig. 4A). Moreover, an inhibitory effect of gefitinib on TNF-α-induced Akt/NF-κB activation was not observed although wortmannin, a phosphatidylinositol 3-kinase inhibitor, completely inhibited this signaling in PC-9/ZD2001 cells (Fig. 4B). These results suggest that the weak effect of EGFR on Akt/NF-κB signaling could occur between EGFR and phosphatidylinositol 3-kinase in PC-9/ZD2001 cells.

Several articles reported that the sensitivity to gefitinib is regulated by active mutant EGFR (30, 31), by the expression level of phosphatase and tensin homologue/MMAC/TEP (32), and by levels of Akt phosphorylation (13, 33, 34). Because the gefitinib-hypersensitive PC-9 cells originally had 15-bp deletion mutation in exon 19 of EGFR, they were thought to have a gefitinib-sensitive active mutant EGFR (35); however, because we found no alteration of the EGFR mRNA sequence in PC-9/ZD2001 cells (data not shown), we conclude that this gefitinib-resistant cell line was a good model for acquired gefitinib resistance. In our previous study, EGFR signaling mediated by transforming growth factor-α, an EGFR ligand, could not activate the mitogen-activated protein signaling pathway but could partially activate the Akt signaling cascade in PC-9/ZD2001. In PC-9/ZD2001R cells, the association between EGFR and mitogen-activated protein kinase signaling was completely reconstituted. On the basis of this result, we conclude that the decrease of EGFR signaling to the mitogen-activated protein kinase signaling pathway might contribute to acquired gefitinib resistance.[5] In this study, TNF-α significantly induced EGFR autophosphorylation but subsequent activation of the Akt signaling cascade was little observed in PC-9/ZD2001 (Fig. 4A and B). This decreased EGFR signaling on Akt could be partially caused by the decrease in EGFR expression but we have

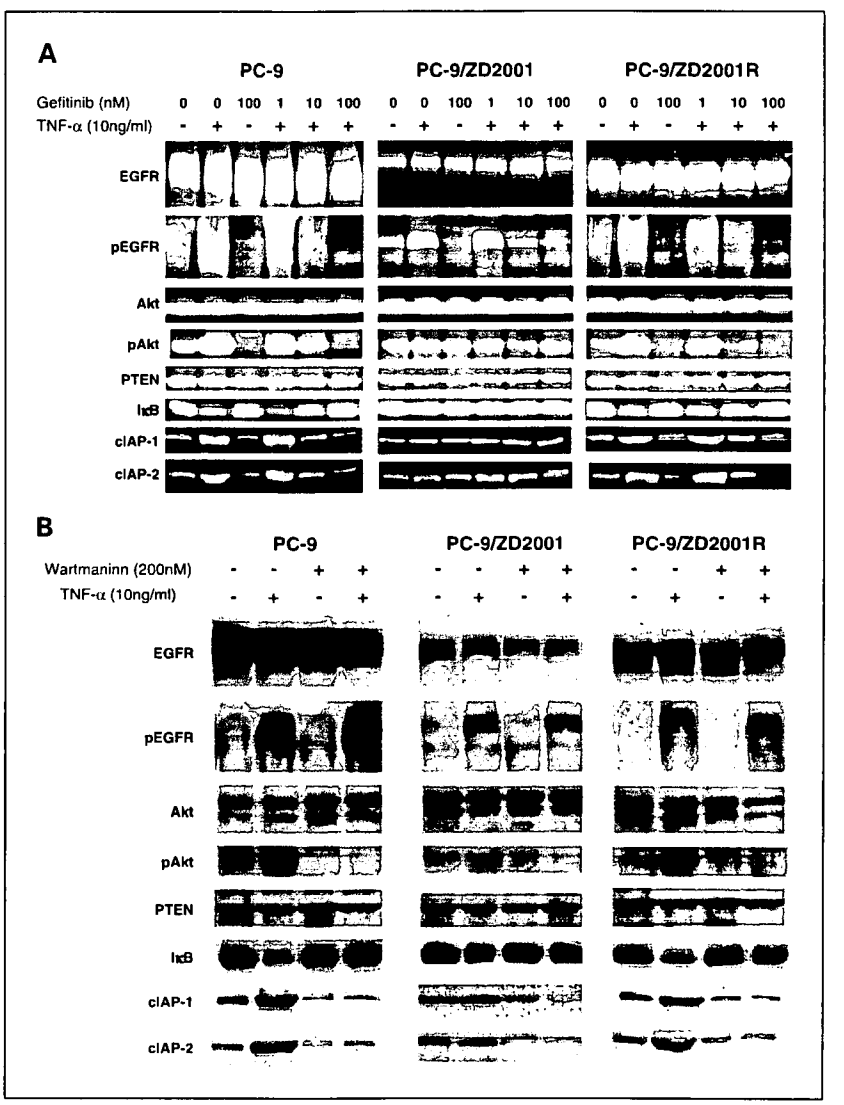

Fig. 4. Inhibitory effect of gefitinib on TNF-α-induced phosphorylation of Akt1 and degradation of IκB. Cells were treated with TNF-α with or without gefitinib (*A*) or wortmannin (*B*) simultaneously for 30 minutes at 37°C. Cell lysates were prepared and equivalent amounts of protein from each cell lysate were resolved with 10% SDS-PAGE, transferred to nitrocellulose membranes, and subjected to Western blotting with specific antibodies (as described in Materials and Methods). The EGFR and Akt1 membranes were stripped and reblotted with antibodies against phospho-EGFR (Tyr1045) and phospho-Akt, respectively. Expression of β-actin was used as internal control. Although treatment with TNF-α significantly phosphorylated EGFR in all three cell lines, downstream Akt/NF-κB activation was observed in PC-9 and PC-9/ZD2001R but weakly in PC-9/ZD2001. Gefitinib inhibited cross-talk signaling in PC-9 and PC-9/ZD2001R cells but not in PC-9/ZD2001 cells (*A*). A phosphatidylinositol 3-kinase inhibitor, wortmannin, completely inhibited this signaling in all three cell lines (*B*).